

The Evolution of Polymorphic Hybrid Incompatibilities in House Mice

Erica L. Larson,^{*,1} Dan Vanderpool,^{*} Brice A. J. Sarver,^{*} Colin Callahan,^{*,2} Sara Keeble,^{*,†}
Lorraine P. Provencio,[†] Michael D. Kessler,[†] Vanessa Stewart,^{*} Erin Nordquist,^{*} Matthew D. Dean,[†]
and Jeffrey M. Good^{*,3}

^{*}Division of Biological Sciences, University of Montana, Missoula, Montana 59812 and [†]Molecular and Computational Biology Section, Department of Biological Sciences, University of Southern California, Los Angeles, California 90089

ORCID ID: 0000-0002-7318-3122 (S.K.)

QA1

ABSTRACT Resolving the mechanistic and genetic bases of reproductive barriers between species is essential to understanding the evolutionary forces that shape speciation. Intrinsic hybrid incompatibilities are often treated as fixed between species, yet there can be considerable variation in the strength of reproductive isolation between populations. The extent and causes of this variation remain poorly understood in most systems. We investigated the genetic basis of variable hybrid male sterility (HMS) between two recently diverged subspecies of house mice, *Mus musculus domesticus* and *Mus musculus musculus*. We found that polymorphic HMS has a surprisingly complex genetic basis, with contributions from at least five autosomal loci segregating between two closely related wild-derived strains of *M. m. musculus*. One of the HMS-linked regions on chromosome 4 also showed extensive introgression among inbred laboratory strains and transmission ratio distortion (TRD) in hybrid crosses. Using additional crosses and whole genome sequencing of sperm pools, we showed that TRD was limited to hybrid crosses and was not due to differences in sperm motility between *M. m. musculus* strains. Based on these results, we argue that TRD likely reflects additional incompatibilities that reduce hybrid embryonic viability. In some common inbred strains of mice, selection against deleterious interactions appears to have unexpectedly driven introgression at loci involved in epistatic hybrid incompatibilities. The highly variable genetic basis to F1 hybrid incompatibilities between closely related mouse lineages argues that a thorough dissection of reproductive isolation will require much more extensive sampling of natural variation than has been commonly utilized in mice and other model systems.

KEYWORDS polymorphism; hybrid male sterility; transmission ratio distortion; QTL mapping; introgression

THE evolution of intrinsic hybrid incompatibilities, whereby divergent genomic regions interact negatively in hybrid genomes, is one of the most commonly studied models of speciation [*i.e.*, Bateson–Dobzhansky–Muller incompatibilities or BDMIs, Bateson 1909; Dobzhansky 1937; Muller 1942; reviewed in Maheshwari and Barbash (2011)]. Although often viewed as fixed epistatic barriers to gene flow

between species, many incompatible alleles are polymorphic within populations, leading to variation in the overall strength of reproductive isolation between populations (Gordon 1927; Patterson and Stone 1952; Forejt and Ivanyi 1974; Reed and Markow 2004; Good *et al.* 2008b; Scopece *et al.* 2010; Cutter 2012). Relatively few studies have examined the genetic basis of variation in BDMIs (Christie and Macnair 1987; Vyskočilová *et al.* 2005; Wright *et al.* 2013; Sweigart and Flagel 2015; Case *et al.* 2016) and the evolutionary forces underlying variable incompatibilities remain unexplored in most species.

Hybrid incompatible alleles can arise through any evolutionary process that contributes to genetic divergence (*e.g.*, genetic drift, natural or sexual selection). However, reproductive isolation is expected to evolve more quickly when divergence is driven by selection. Consistent with this, several incompatibility genes show signatures of positive

Copyright © 2018 by the Genetics Society of America

doi: <https://doi.org/10.1534/genetics.118.300840>

Manuscript received February 20, 2018; accepted for publication April 23, 2018; published Early Online April 24, 2018.

Supplemental material available at Figshare: <https://doi.org/10.25386/genetics.6149399>.

¹Present address: Department of Biological Sciences, University of Denver, Denver, CO 80210.

²Present address: Center for Epigenetics, Johns Hopkins University School of Medicine, Baltimore, MD 21205.

³Corresponding author: Division of Biological Sciences, University of Montana, 32 Campus Drive, HS104, Missoula, MT 59812. E-mail: jeffrey.good@umontana.edu

73 selection or have diverged through antagonistic coevolution-
74 ary dynamics (Johnson 2010; Presgraves 2010; Maheshwari
75 and Barbash 2011). Polymorphism is an inevitable phase in
76 the fixation of an allele, but directional selection should fix
77 alleles relatively quickly. Thus, it should be rare that incompatibilities are sampled while polymorphic if positive directional selection drives the evolution of BDMS. Alternatively, BDMS could involve a combination of unsorted ancestral variation or modifying loci that segregate neutrally within species (Rieseberg and Blackman 2010; Scopece *et al.* 2010; Cutter 2012; Matute *et al.* 2014) or are subject to balancing selection (Cutter 2012). Finally, polymorphic incompatibilities may reflect the breakdown of reproductive barriers due to gene flow between partially isolated populations. Hybrid incompatible alleles are generally assumed to be resistant to introgression (Barton and Hewitt 1985; Harrison 1990; Payseur 2010), but epistatic barriers may quickly erode in the face of gene flow (Bank *et al.* 2012; Lindtke and Buerkle 2015). Differentiating between these alternatives is crucial to understanding the evolution of reproductive isolation and the nature of species boundaries.

79 House mice provide a powerful system to understand the
80 causes of polymorphic barriers during the early stages of
81 speciation. There are three major lineages within *Mus mus-*
82 *culus*—*M. m. musculus*, *M. m. domesticus*, and *M. m. casta-*
83 *neus*—that diverged ~0.35–0.50 MYA (Gerald *et al.* 2011)
84 and show partial reproductive isolation primarily due to hybrid male sterility (HMS). However, there appears to be considerable standing genetic variation for the strength of HMS (Britton-Davidian *et al.* 2005; Vyskočilová *et al.* 2005; Good *et al.* 2008b; Turner *et al.* 2012). For example, crosses between *M. m. musculus* females and *M. m. domesticus* males typically yield sterile F1 hybrid males due, in part, to negative interactions between *M. m. musculus* Chr X and the autosomal gene *Prdm9*, a DNA binding protein that directs the location of double-strand breaks during recombination (Mihola *et al.* 2009). PRDM9 binding sites evolve rapidly (Baker *et al.* 2015), leading to asymmetric binding and autosomal asynapsis that disrupts sex chromosome expression during spermatogenesis (Bhattacharyya *et al.* 2013; Campbell *et al.* 2013; Turner *et al.* 2014; Davies *et al.* 2016; Larson *et al.* 2017). *Prdm9* appears to be polymorphic for sterile and fertile alleles within both *M. m. domesticus* and *M. m. musculus* (Forejt and Ivanyi 1974; Vyskočilová *et al.* 2009; Flachs *et al.* 2012), and the strength of *Prdm9*-associated sterility is variable within *M. m. musculus* (Bhattacharyya *et al.* 2014; Flachs *et al.* 2014; Turner *et al.* 2014).

85 There is also variation in the severity of HMS in house mice
86 that is independent of the *M. m. musculus* X (Good *et al.*
87 2008b). For example, crosses between *M. m. domesticus* fe-
88 males and *M. m. musculus* males produce sterile or fertile
89 hybrid males dependent on the genotype of the *M. m. mus-*
90 *culus* sire (Vyskočilová *et al.* 2005; Good *et al.* 2008b;
91 Bhattacharyya *et al.* 2014; Flachs *et al.* 2014). The autosomal
92 variants contributing to HMS in these crosses are unresolved
93 and, aside from the rapid evolution of *Prdm9* (Davies *et al.*

2016), the causes of standing variation for HMS are not clear.
One possible factor is that the small effective population sizes
of house mice results in strong genetic drift and local inbreeding (Gerald *et al.* 2011). Further, *M. m. domesticus* and *M. m. musculus* form a narrow hybrid zone in central Europe (Janoušek *et al.* 2012), which may weaken reproductive barriers through introgression (Turner and Harr 2014).

In this study, we used the genetic variation segregating between two wild-derived inbred strains of *M. m. musculus* to begin to characterize the genetic architecture of polymorphic barriers between *M. m. domesticus* females and *M. m. musculus* males. We found that polymorphic HMS encompasses at least five autosomal regions of the genome. We then used additional genetic crosses, whole genome sequencing of sperm pools, and population genomic analyses to explore the mechanistic and evolutionary drivers contributing to variation at one of these regions on the distal portion of Chr 4. These diverse genetic and genomic experiments further reveal the complex genetic basis of reproductive isolation in this system and demonstrate how these reproductive barriers have shaped introgression among mouse subspecies and the genomic composition of common laboratory strains of mice.

Materials and Methods

Mouse strains and experimental crosses

We focused on two wild-derived inbred strains of *M. m. musculus* (PWK/PhJ and CZECHII/EiJ, hereafter *musculus*^{PWK} and *musculus*^{CZII}) that differ in the degree of HMS when crossed to *M. m. domesticus* (Good *et al.* 2008b). The *musculus*^{PWK} strain was originally isolated near the hybrid zone in Prague, Czechia (50.0216°N, 14.4350°E) and yields weak HMS when crossed to female *M. m. domesticus*. The *musculus*^{CZII} was isolated further from the hybrid zone in Bratislava, Slovakia (48.1492°N, 17.1070°E) and produces mostly sterile males when crossed to female *M. m. domesticus*. We used two wild-derived strains of *M. m. domesticus* (WSB/PhJ and LEWES/PhJ, hereafter *domesticus*^{WSB} and *domesticus*^{LEW}) derived from natural populations in North America (MD, 39.3358°N, 77.3282°W and DE, 39.1453°N, 75.4188°N). Mice were originally purchased from Jackson Laboratory (Bar Harbor, ME). All animal use was approved by the University of Montana (protocol 002–13) and the University of Southern California (protocol 11,394) Institutes for Animal Care and Use Committees.

Hybrid incompatibilities underlying F1 hybrid phenotypes usually cannot be mapped because of a lack of genetic variation. However, the existence of polymorphic sterility factors within *musculus* provides an elegant way to resolve these incompatibilities directly in F1 hybrid males. We first quantified HMS in F1 crosses between female *domesticus*^{WSB} and either *musculus*^{PWK} or *musculus*^{CZII} males. To control for the effects of inbreeding depression in inbred strains, we compared the fertility of these F1 hybrids to *M. m. domesticus* interstrain F1 males (*domesticus*^{WSB} × *domesticus*^{LEW}),

185 evaluating each cross at different time points [60–65, 70–80, 186 and 85–95 days postpartum (dpp)]. We then used an F1 187 hybrid test cross between *domesticus*^{WSB} females and inter- 188 strain F1 males from reciprocal crosses of *musculus*^{PWK} and 189 *musculus*^{CZII} (Figure 1). This design maintains the F1 hybrid 190 genotype, while segregating variation between two different 191 *M. m. musculus* genomes. Finally, we backcrossed *M. m. mus-* 192 *culus* interstrain F1 males to *musculus*^{PWK} females to deter- 193 mine if loci on Chr 4 showing strong transmission ratio 194 distortion (TRD) in our hybrid crosses also showed TRD 195 within *M. m. musculus*.

196 **Male reproductive phenotypes**

198 We quantified reproductive phenotypes of virgin males 199 weaned in same-sex sibling groups at 21 dpp and housed 200 singly at 45 dpp to mitigate dominance interactions (Snyder 201 1967). Males were killed using carbon dioxide followed by 202 cervical dislocation at 58–70 dpp (F1 hybrid test cross) or up 203 to 90 dpp (aged F1 males). Following Good *et al.* (2008b), we 204 measured paired testes (an overall measure of fertility) and 205 seminal vesicles (correlated with serological testosterone lev- 206 els) relative to body weight. We isolated sperm from caudal 207 epididymides diced in 1 ml of Dulbecco's PBS (Sigma, St. 208 Louis, MO) and incubated at 37° for 10 m. The proportion 209 of motile sperm and total sperm numbers were estimated 210 from 5 µl suspensions (regular and heat-shocked, respec- 211 tively) viewed in a Makler counting chamber on a light mi- 212 croscope over a fixed area and observation time. To evaluate 213 sperm morphology, 25 µl sperm suspensions were fixed and 214 stained, and ≥100 intact sperm were visually classified by a 215 single individual (E.L.L.) while blind to genotype. Sperm head 216 morphology were (1) normal with a long apical hook, (2) 217 slightly abnormal (*i.e.*, shortened hook), (3) abnormal (*i.e.*, 218 short hook and rounded shape), or (4) severely abnormal (*i.* 219 *e.*, amorphous shape). We summarized these categories with a 220 weighted index that ranged from high (3) to low (0) quality 221 sperm (Oka *et al.* 2004; Good *et al.* 2008a). Sperm tail mor- 222 phology were (1) normal, (2) bent at the base of the sperm 223 head, (3) bent in the center of the tail forming a loop, or (4) 224 twisted distally (White *et al.* 2011).

225 **Genotyping and genome sequencing**

227 We genotyped 468 individuals from our two genetic mapping 228 experiments (*i.e.*, 156 F1 hybrid test cross males and 312 *M.* 229 *m. musculus* backcross) and eight reference samples (two of 230 each parent strain and *domesticus*^{WSB} × *musculus*^{CZII} F1 hy- 231 brids) using double-digest restriction site-associated DNA 232 sequencing (ddRADseq; Peterson *et al.* 2012), with minor 233 modifications. DNA was extracted from liver tissue using 234 the NucleoSpin Tissue kit (Machery-Nagel, Düren, Germany) 235 and incubated in 5 µl RNAase A (Fisher Scientific, Waltham, 236 MA) at 37° for 15 m. We digested 1 µg of DNA with *MspI* and 237 *SbfI*-HF enzymes (New England Biolabs, Beverly, MA), li- 238 gated unique adaptors, and selected 200–500 bp fragments 239 using a two-step size selection with AMPure XP beads (Agen- 240 court Bioscience, Beverly, MA). Individual libraries were am-

plified 16 cycles in three 20 µl reactions using Phusion High- 241 Fidelity DNA Polymerase (New England BioLabs), cleaned 242 using AMPureXP, and quantified with a NanoPhotometer 243 (IMPLEN, München, Germany). F1 hybrid libraries were 244 paired-end sequenced on an Illumina HiSequation 2000 at 245 the QB3, University of California, Berkley and on a MiSeq at 246 the IBEST Genomic Resources Core, University of Idaho. The 247 *M. m. musculus* backcross libraries were single-end se- 248 quenced on an Illumina HiSequation 4000 at the University 249 of Oregon Genomics and Cell Characterization Core Facility. 250

251 Libraries were checked for intact barcodes, restriction 252 enzyme cut-sites, and demultiplexed using *preprocess_radta-* 253 *g_lane.py* (Peterson *et al.* 2012). We used Trimmomatic 254 v0.32 (Lohse *et al.* 2012) to remove adaptor sequences and 255 low-quality bases and mapped reads to the Genome Refer- 256 ence Consortium mouse build 38 (GRCm38) using BWA- 257 MEM v0.7.10 (Li 2013). We applied the Genome Analysis 258 Tool Kit (GATK) v3.4 (McKenna *et al.* 2010) to call SNPs 259 (HaplotypeCaller) that we then filtered (minDP 10, maxDP 260 150, minGQ 20) using VCFtools v0.1.14 (Danecek *et al.* 261 2011). We retained biallelic SNPs that were homozygous in 262 the parent references, heterozygous in the F1 hybrid refer- 263 ence, genotyped in ≥95% of individuals, and >1000 bp from 264 other SNPs. We retained individuals that were genotyped 265 in ≥85% of markers and showed normal crossover rates.

266 We also performed two targeted genotyping assays. Males 267 from the F1 hybrid test cross were genotyped for microsatellite 268 length variants that encompass different *Prdm9* alleles. We 269 used modified versions of D17Mit78 (forward: CACAGT- 270 GAGTCTGGGCTAGTC, reverse: GCATCTTATGGATTGAAA- 271 TACGG) and D17Mit261 (forward: CCCTTGCTCTCCT- 272 TCATTCA, reverse: AATGCCAAATGGTCAGCC; Copeland 273 *et al.* 1993) in 10 µl PCR reactions using MangoTaq (Bioline, 274 Luckenwalde, Germany), run at 35 cycles of 94° for 30 sec, 275 58–48° for 30 sec (decreased by 1° per cycle for the first 276 10 cycles), and 72° for 1 m. We also expanded the genotyping 277 of our *M. m. musculus* backcross using diagnostic microsatel- 278 lites from the middle (D4Mit64: 140.08–141.03 bp) and distal 279 end (D4Mit127: 148.60–151.60 bp) of Chr 4 (Copeland 280 *et al.* 1993). These markers spanned SNPs genotyped using 281 ddRADseq, and we genotyped 88 mice using both methods to 282 allow cross validation. All fragments were analyzed on an ABI 283 3130xl at the University of Montana Genomics Core.

284 Reference genomes have been published for *musculus*^{PWK} 285 and *domesticus*^{WSB} (Keane *et al.* 2011). We generated whole 286 genome shotgun sequences of a female *musculus*^{CZII} and a 287 female *domesticus*^{LEW} from NEXTflex DNA sequencing geno- 288 mic libraries (Bio Scientific, Austin, TX) that were paired-end 289 sequenced on an Illumina HiSequation 2000 at the QB3 Uni- 290 versity of California, Berkley. We generated additional whole 291 genome sequence data from the same *musculus*^{CZII} female at 292 GENEWIZ (South Plainfield, NJ) using Illumina TruSeq li- 293 braries, paired-end sequenced on an Illumina HiSequation 294 2500. These data were processed as described above. 295

297
298
299
300
301
302
303
304
305
306
307
308
309
310
311
312
313
314
315
316
317
318
319
320
321
322
323
324
325
326
327
328
329
330
331
332
333
334
335
336
337
338
339
340
341
342
343
344
345
346
347
348
349
350
351
352

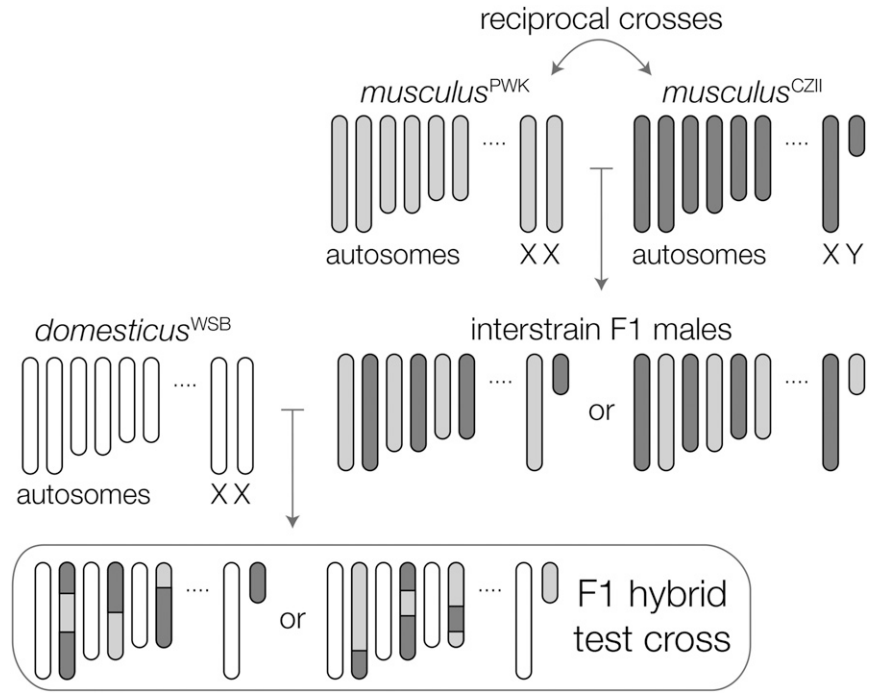


Figure 1 Crossing design to map polymorphic HMS loci in *musculus*. The fertility of F1 hybrids from crosses between *M. m. domesticus* females and *M. m. musculus* males depends on the strain of *M. m. musculus*; hybrids with *musculus*^{CZII} sires have more severe sterility. We test crossed interstrain *M. m. musculus* F1s to *M. m. domesticus* females to map F1 hybrid sterility alleles segregating within *M. m. musculus*.

353
354
355
356
357
358
359
360
361
362
363
364
365
366
367
368
369
370
371
372
373
374
375
376
377
378
379
380
381
382
383
384
385
386
387
388
389
390
391
392
393
394
395
396
397
398
399
400
401
402
403
404
405
406
407
408

QTL mapping

We performed QTL mapping in R/qtl v1.40-8 (Broman *et al.* 2003) with an assumed genotyping error rate of 0.001 and the Carter–Falconer mapping function (Carter and Falconer 1951). For all QTL analyses we used a grid size of 1 cM and 5% genome-wide significance thresholds estimated from 1000 permutations. We used standard interval QTL interval mapping (*scanone*) with a Haley–Knott regression for normally distributed traits, and nonparametric interval mapping for the proportion of motile sperm, and sperm head and tail morphologies. We used two-dimensional QTL mapping (*scantwo*) and multiple QTL model selection (*stepwiseqtl*) to identify additional QTL that may be involved in epistatic interactions. Multiple QTL models were compared using penalized LOD score with thresholds calculated from *scantwo* permutations. We tested for TRD in our cross using a χ^2 test of Mendelian proportions.

Genomic analyses

To investigate the evolutionary history of genomic regions associated with polymorphic sterility, we first analyzed the newly sequenced *musculus*^{CZII} and *domesticus*^{LEW} genomes and published genomic data from GRCm38 (*domesticus*^{C57}), *domesticus*^{WSB}, *musculus*^{PWK}, and *Mus spretus* SPRET/EiJ (Keane *et al.* 2011). For each genome, we called SNPs using the GATK (HaplotypeCaller) and filtered SNPs with VCFtools (minDP 10, maxDP 150, minGQ 30). We generated a BED file with all SNP positions and used the GATK to re-call genotypes in each genome for our target SNPs (HaplotypeCaller) and filter VCFs (SelectVariants, minGQ 30, biallelic). We then tested for introgression using the four-taxon *D*-statistic (Green *et al.* 2010; Durand *et al.* 2011) as implemented in dfoil (Pease and Hahn 2015). Here, the *D*-statistic is the nor-

malized difference in site pattern counts that support a closer relationship between *musculus*^{CZII} and a focal *M. m. domesticus* (ABBA, negative *D*-statistic) or *musculus*^{PWK} and a focal *M. m. domesticus* (BABA, positive *D*-statistic) with variants polarized using *M. spretus*. We calculated the *D*-statistic per chromosome and for nonoverlapping 100 kb and 1 Mb windows. We repeated these analyses using three different strains of *M. m. domesticus* (*domesticus*^{C57}, *domesticus*^{WSB}, and *domesticus*^{LEW}).

Second, we used published genotype data for classic laboratory strains, wild-derived strains (Yang *et al.* 2011), and wild populations of house mice (Harr *et al.* 2016) to evaluate genetic structure with principal components analysis using the R package *SNPRelate* (Zheng *et al.* 2012). We then used genotype data from 76 classic laboratory strains (Yang *et al.* 2011) to test for gametic disequilibrium (r^2) between candidate sterility regions and SNPs on other chromosomes using PLINK v2.0 (Chang *et al.* 2015). We restricted these analyses to SNPs between *musculus*^{PWK} and *musculus*^{CZII} ≥ 1 Mb apart with no missing data, minor allele frequencies ≥ 0.1 , and that were also fixed between strains of *M. m. musculus* (CZECHII, STUS, and STUP) and *M. m. domesticus* (LEWES, ZALENDE, and PERA) with very low levels of introgression (Yang *et al.* 2011; Didion and Pardo-Manuel de Villena 2012).

Third, we evaluated phylogenetic discordance using whole exome data from 10 species of *Mus* (Sarver *et al.* 2017) and whole genomes from *domesticus*^{C57} and *domesticus*^{WSB} (Keane *et al.* 2011). We cleaned and mapped reads to species-specific exome-pseudoreferences generated by Sarver *et al.* (2017). We used the MPI version of RAxML v8.2.3 (Stamatakis 2014) to estimate maximum likelihood phylogenies (rapid bootstrapping and a GTR + Γ model of sequence evolution) for nonoverlapping 100 kb windows, and used

409
410
411
412
413
414
415
416
417
418
419
420
421
422
423
424
425
426
427
428
429
430
431
432
433
434
435
436
437
438
439
440
441
442
443
444
445
446
447
448
449
450
451
452
453
454
455
456
457
458
459
460
461
462
463
464

Table 1 Reproductive phenotypes for *M. m. domesticus* and hybrid males

	F1 hybrids			F1 hybrid test cross		
	<i>domesticus</i> ^{WSB} × <i>domesticus</i> ^{LEW}	<i>domesticus</i> ^{WSB} × <i>musculus</i> ^{PWK}	<i>domesticus</i> ^{WSB} × <i>musculus</i> ^{CZII}	<i>domesticus</i> ^{PWK} × <i>musculus</i> ^{PWK}	<i>domesticus</i> ^{WSB} × <i>musculus</i> ^{CZII}	<i>domesticus</i> ^{WSB} × <i>musculus</i> ^{CZII} × <i>PWK</i>
Sample size	21	28	30	78	78	78
Body weight (g)	17.32 ± 3.1e-01	18.26 ± 4.6e-01	17.15 ± 2.8e-01	18.39 ± 2.8e-01	17.87 ± 2.1e-01	17.87 ± 2.1e-01
Relative paired testis weight (mg/g)	11.5 ± 2.9e-01	7.5 ± 1.5e-01 ▼	6.2 ± 1.3e-01 ▼	6.6 ± 1.3e-01 ▼	6.95 ± 1.6e-01 ▼	6.95 ± 1.6e-01 ▼
Relative paired seminal vesicle weight (mg/g)	5.25 ± 3.7e-01	6 ± 2.2e-01 ▲	5.8 ± 1.7e-01	5.9 ± 1.4e-01 ▲	5.6 ± 1.1e-01	5.6 ± 1.1e-01
Proportion motile sperm	0.77 ± 3.1e-02	0.83 ± 1.9e-02	0.77 ± 3.4e-02	0.84 ± 1.6e-02 ▲	0.83 ± 2.7e-02 ▲	0.83 ± 2.7e-02 ▲
Sperm count (1 × 10 ⁶)	19.4 ± 1.5e+00	11.8 ± 1.6e+00 ▼	5.8 ± 9.6e-01 ▼	4.9 ± 4.2e-01 ▼	5.7 ± 4.2e-01 ▼	5.7 ± 4.2e-01 ▼
Sperm head morphology index	2.99 ± 4.7e-03	2.84 ± 2e-02 ▼	1.14 ± 4.8e-02 ▼	2.43 ± 6.6e-02 ▼	2.18 ± 7.6e-02 ▼	2.18 ± 7.6e-02 ▼
Proportion normal sperm head attachment	1 ± 8.8e-04	0.99 ± 2.7e-03 ▼	0.96 ± 6.2e-03 ▼	0.99 ± 2.8e-03 ▼	0.98 ± 4.4e-03 ▼	0.98 ± 4.4e-03 ▼
Proportion straight proximal sperm tail	0.97 ± 6.9e-03	0.96 ± 4.6e-03 ▼	0.99 ± 4.2e-03 ▲	0.97 ± 2.5e-03	0.96 ± 3e-03	0.96 ± 3e-03
Proportion straight distal sperm tail	1 ± 3.1e-03	1 ± 2.6e-03	1 ± 3.4e-03	0.99 ± 1.5e-03 ▼	0.99 ± 1.9e-03 ▼	0.99 ± 1.9e-03 ▼

Only F1 hybrids between 58 and 70 days postpartum (dpp) are included to allow direct comparison with the F1 hybrid test cross. See Figure S1 for reproductive traits across an F1 hybrid's reproductive lifespan. Traits are summarized as median values (±SE), and arrows represent significant increase (▲) or decrease (▼) in trait values relative to the *M. m. domesticus* control cross. Values in bold are significantly different between F1 hybrids (Wilcoxon test, false discovery rate-corrected $P \leq 0.05$). Trait proportions are polarized so that higher values indicate higher quality reproductive traits.

these windows to produce a concatenated species tree for each chromosome. We then used ASTRAL v4.10.11 (Mirarab and Warnow 2015) to estimate the species tree while accounting for phylogenetic discordance among individually estimated gene trees. Trees were visualized with FigTree v1.4.3.

Genome-wide assessment of TRD

To test for TRD associated with sperm function, we used low-coverage whole genome sequencing of motile and immotile sperm populations collected from four F1 male *M. m. musculus* (*musculus*^{PWK} × *musculus*^{CZII}). Epididymal sperm were collected from killed adult males (106 dpp) in 2 ml Dulbecco's PBS (equilibrated at 37° and 5% carbon dioxide overnight). We applied 1 ml aliquots of sperm to a Percoll gradient (1 ml layers of 90 and 45% Percoll at 37°; GE Healthcare Life Sciences) and centrifuged (300 g for 13 min) to separate cellular debris (top), immotile sperm (middle), and motile sperm (bottom) (Ng *et al.* 1992; Phelps *et al.* 1999). Immotile and motile sperm fractions (400 µl each) were rinsed (1 ml 1.5 M NaCl, centrifuged at 10,000 g for 10 min) and stored at -80°. We purified DNA using the MasterPure Complete DNA purification kit (Epicentre Biotechnologies). Sperm fractions were rinsed in 600 µl of 70% EtOH (centrifuged at 14,000 g for 5 min) and incubated overnight at 55° in 600 µl lysis buffer, 25 µl of 1 M dithiothreitol, and 10 µl of 20 mg/ml proteinase K. We treated samples with RNase A (3 µl, for 30 min at 37°), precipitated the sperm in 200 µl of protein precipitation buffer (centrifuged at 14,000 g for 30 min), and incubated in 600 µl of isopropanol at -80° for 2-3 hr (centrifuged at 14,000 g for 20 min). The pellet was rinsed with 500 µl 75% ethanol (centrifuged at 14,000 g for 10 min) and dried overnight. We then constructed sequencing libraries using the NEBNext Ultra DNA Library Prep Kit for Illumina with Bio Scientific NEXTflex DNA Barcodes and generated 76 bp paired-end sequences on a HiSeq4000 at the Epigenome Center, University of Southern California.

We conducted all analyses using reads mapped to strain-specific pseudoreferences for *musculus*^{CZII} or *musculus*^{PWK} (Sarver *et al.* 2017). Briefly, for each whole genome (described above), we called SNPs relative to GRCm38 (GATK HaplotypeCaller), hard-filtered our SNPs (maskExtension 5, QD < 2.0, FS > 60.0, MQ < 40.0, MQRankSum < -12.5, ReadPosRankSum < -8.0, QUAL < 30.0, minDP 10, maxDP 150), recalled SNPs that passed filtering at a base-pair resolution in each genome, and used this high-confidence SNP set to inject variants into GRCm38 using the GATK FastaAlternativeReferenceMaker. We trimmed and quality-filtered sperm fraction reads using expHTS (Streett *et al.* 2015), mapped reads to each pseudoreference using BWA-MEM, and called SNPs using the GATK (HaplotypeCaller). We assigned reads (MQ ≥ 56) that overlapped at least one diagnostic SNP as either *musculus*^{PWK} or *musculus*^{CZII} origin, and summarized read counts in 1 Mb sliding windows (step size 0.5 Mb). We tested for TRD in windows with ≥100 reads in all samples using a χ^2 test (false discovery rate-corrected $P < 0.01$;

465
466
467
468
469
470
471
472
473
474
475
476
477
478
479
480
481
482
483
484
485
486
487
488
489
490
491
492
493
494
495
496
497
498
499
500
501
502
503
504
505
506
507
508
509
510
511
512
513
514
515
516
517
518
519
520

521
522
523
524
525
526
527
528
529
530
531
532
533
534
535
536
537
538
539
540
541
542
543
544
545
546
547
548
549
550
551
552
553
554
555
556
557
558
559
560
561
562
563
564
565
566
567
568
569
570
571
572
573
574
575
576

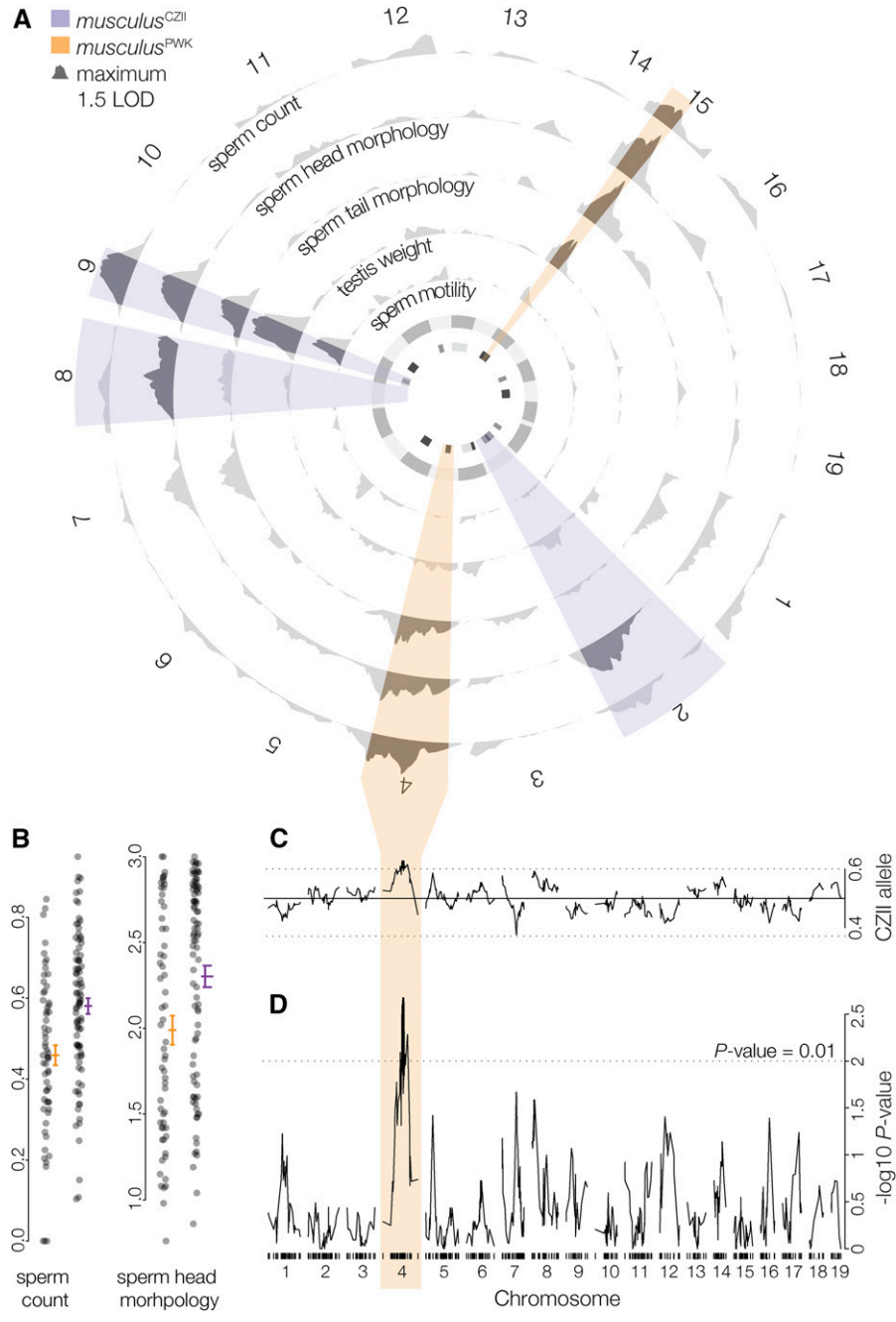


Figure 2 QTL for polymorphic HMS in *musculus*. (A) LOD curves (standard interval mapping) for HMS phenotypes. Highlighted intervals are the maximum LOD intervals (across all traits) on each chromosome for QTL associated with lower fertility in *musculus*^{CZII} (purple) and *musculus*^{PWK} (orange). The inner circle is QTL LOD support intervals for previously reported hybrid sterility loci mapped in *M. m. domesticus* and *M. m. musculus* F2 crosses (White *et al.* 2011; Turner *et al.* 2014; medium gray), and an F1 hybrid test cross (Bhattacharyya *et al.* 2014; light gray). (B) Normalized sperm count and sperm head morphology index plotted against the genotype of the marker with the largest Chr 4 LOD score. Lines indicate mean trait values (±SE). (C) Frequency of the *musculus*^{CZII} allele at each marker (Mendelian expectations 0.5:0.5, genome wide average: 0.496:0.504). (D) TRD plotted as the $-\log_{10} P$ -value from χ^2 test for Mendelian segregation per chromosome. Tick marks indicate SNP positions.

577
578
579
580
581
582
583
584
585
586
587
588
589
590
591
592
593
594
595
596
597
598
599
600
601
602
603
604
605
606
607
608
609
610
611
612
613
614
615
616
617
618
619
620
621
622
623
624
625
626
627
628
629
630
631
632

Benjamini and Hochberg 1995) to test the proportions of *musculus*^{PWK} vs. *musculus*^{CZII} reads in motile vs. immotile sperm fractions. We considered a window skewed if the proportion of *musculus*^{CZII}-derived reads significantly differed by at least 0.15 between sperm fractions.

To validate our Percoll method, we repeated our pipeline with experimentally combined normal and heat-shocked (immotile) sperm samples from two predominantly *M. m. domesticus* inbred strains (C57BL/6J and DBA/2J). We pooled normalized sperm extractions from each strain and then mixed sperm in equal proportions from the two strains, and repeated our experiment to vary which strain was heat shocked. We isolated DNA as described above, and

PCR-amplified and Sanger-sequenced through a marker containing a diagnostic SNP.

Data availability

All data are available through NCBI under projects SRP093943 (F1 hybrid test cross RADseq), SRP094878 (*M. m. musculus* CZECHII/EiJ whole genome sequencing), SRP094877 (*M. m. domesticus* LEWES/EiJ whole genome sequencing), SRP082237 (sperm pools whole genome sequencing), and SPR102485 (backcross RADseq). Supplemental Material, File S1 contains phenotype data for F1 hybrids and F1 hybrid test cross. File S2 contains microsatellite genotypes for markers inside and outside the Chr 4 TRD

633
634
635
636
637
638
639
640
641
642
643
644
645
646
647
648
649
650
651
652
653
654
655
656
657
658
659
660
661
662
663
664
665
666
667
668
669
670
671
672
673
674
675
676
677
678
679
680
681
682
683
684
685
686
687
688

Table 2. Polymorphic hybrid sterility QTL detected using standard interval QTL mapping

	Chr	Position (cM)	LOD score	P-value	Position (Mb)	1.5 LOD interval (Mb)	%Var ^a	Effect ^b	Phenotype means ± SE	
									<i>musculus</i> ^{PWK}	<i>musculus</i> ^{CZII}
Relative paired testis weight (mg/g)	9	36.49	4.79	0.001	92.81	49.08–113.49	11.22	-0.88	7.3 ± 0.13	6.34 ± 0.15
	15	22.74	3.12	0.023	78.25	29.87–84.06	6.9	0.69	6.49 ± 0.14	7.28 ± 0.15
Proportion motile sperm ^c	9	35.49	3.11	0.012	88.11	73.06–122.96	6.42	-0.1	0.84 ± 0.02	0.74 ± 0.02
Normalized sperm count ^d	4	41.82	3.25	0.031	125.29	90.72–155.46	9.83	0.12	0.46 ± 0.02	0.58 ± 0.02
	9	36.49	3.03	0.051	92.81	59.96–111.01	8.77	-0.12	0.58 ± 0.02	0.47 ± 0.02
Sperm head morphology index	2	75.42	3.06	0.023	174.03	148.24–198.11	5.03	-0.29	2.37 ± 0.07	1.97 ± 0.07
	4	67.84	2.87	0.041	154.51	4.17–180.22	3.62	0.25	1.95 ± 0.08	2.33 ± 0.06
	8	45.05	2.86	0.042	113.45	58.94–169.42	7.03	-0.34	2.38 ± 0.08	2.02 ± 0.07
	9	41.49	3.21	0.015	105.4	64.49–122.96	5.98	-0.32	2.38 ± 0.07	1.96 ± 0.07
Proportion normal sperm head attachment ^c	15	22.74	4.94	<0.001	78.25	44.19–84.06	8.48	0.38	1.95 ± 0.07	2.43 ± 0.07
	4	65.23	2.76	0.061	152.74	4.17–180.22	5.75	0.02	0.96 ± 0.004	0.98 ± 0.004
	9	42.49	2.69	0.069	106.53	64.50–122.96	3.77	-0.01	0.98 ± 0.004	0.96 ± 0.004
	15	22.15	4.85	<0.001	77.78	71.46–86.98	7.13	0.02	0.96 ± 0.004	0.98 ± 0.004

^a The percent of the phenotypic variance explained by the QTL, calculated using Haley-Knott regression.
^b The difference between the phenotype averages of the *musculus*^{PWK} and *musculus*^{CZII} alleles. A negative effect indicates the *musculus*^{CZII} allele lowers the reproductive phenotype value. Effects were estimated using Haley-Knott regression.
^c Phenotypes were analyzed using nonparametric interval mapping and %var and effect were estimated using standard interval mapping.
^d Square-root transformed sperm count (1 × 10⁶).

region. Supplemental material available at Figshare: <https://doi.org/10.25386/genetics.6149399>.

Results

HMS is polymorphic and polygenic in *M. m. musculus*

We found that F1 *M. m. domesticus* × *M. m. musculus* hybrids had variable fertility that was dependent on the strain of *M. m. musculus* sires (Table 1), extending previous results (Good *et al.* 2008b). Compared to fertile *M. m. domesticus* F1 males (*domesticus*^{WSB} × *domesticus*^{LEW}), hybrid males with *musculus*^{PWK} sires had smaller testes and more abnormal sperm morphologies. Hybrid males with *musculus*^{CZII} sires were even more severely sterile. These males had smaller testes, lower sperm counts, and a high proportion of abnormal sperm head and tail morphologies compared to hybrid males with *musculus*^{PWK} sires (Table 1). The fertility of *domesticus*^{WSB} × *musculus*^{PWK} hybrids was lower than previously reported from *domesticus*^{LEW} × *musculus*^{PWK} crosses (Good *et al.* 2008b; Campbell *et al.* 2013; Larson *et al.* 2017), suggesting that *domesticus*^{WSB} has sterility factors not present in other strains of *M. m. domesticus* (Odet *et al.* 2015). Differences among F1 crosses remained qualitatively consistent as males aged and sperm head morphology actually worsened with age (Figure S1). Therefore, HMS was not due to delayed reproductive maturity, as has been observed in other crosses (Campbell and Nachman 2014; Flachs *et al.* 2014). Overall, we found that *M. m. domesticus* × *M. m. musculus* HMS was dependent on the paternal strain, indicating autosomal and/or Y-linked sterility loci contribute to polymorphic sterility in *M. m. musculus*.

Next, we used an F1 hybrid test cross to generate 156 males (62 litters) that ranged from reproductively normal to mostly sterile. On average these males had smaller testes, lower sperm counts, and more abnormal sperm head and tail morphologies (Table 1). After filtering for coverage, we retained ddRADseq data for 150 males that had between 118,000 and 921,000 uniquely mapped paired reads (median 297,634, total mapped reads of 48.5 million paired reads). We constructed a genetic map using 582 high-quality SNPs between *musculus*^{CZII} and *musculus*^{PWK}. Using standard interval mapping we detected two regions of the *M. m. musculus* genome on Chr 9 and Chr 15 that contributed to multiple sterility phenotypes (Figure 2A), suggesting a shared genetic and/or developmental basis. Chr 9 QTL reduced the fertility of hybrids carrying a *musculus*^{CZII} allele and Chr 15 QTL reduced the fertility of hybrids carrying a *musculus*^{PWK} allele (Table 2). We identified two additional QTL on Chr 2 and Chr 8 that contributed to abnormal sperm head morphologies associated with the *musculus*^{CZII} allele, and QTL on Chr 4 that contributed to lower sperm counts and abnormal sperm head and tail morphologies associated with the *musculus*^{PWK} allele (Figure 2B). Using two-dimensional QTL mapping, we identified pairs of QTL that additively contributed to sperm count (Chr 4 and Chr 9) and abnormal sperm head morphologies

689
690
691
692
693
694
695
696
697
698
699
700
701
702
703
704
705
706
707
708
709
710
711
712
713
714
715
716
717
718
719
720
721
722
723
724
725
726
727
728
729
730
731
732
733
734
735
736
737
738
739
740
741
742
743
744

745
746
747
748
749
750
751
752
753
754
755
756
757
758
759
760
761
762
763
764
765
766
767
768
769
770
771
772
773
774
775
776
777
778
779
780
781
782
783
784
785
786
787
788
789
790
791
792
793
794
795
796
797
798
799
800

Table 3 Polymorphic F1 hybrid sterility QTL detected using multiple QTL mapping

	Chr	Position (cM)	LOD score	P-value	Position (Mb)	1.5 LOD interval (Mb)	%Var		
							QTL ^a	Full ^b	Effect ± SE ^c
Relative paired testis weight (mg/g)	9	34.65	4.71	<0.001	85.99	59.96–113.49	13.46	NA	-0.96 ± 0.20
Normalized sperm count ^d	4	41.82	3.7	<0.001	125.29	90.72–155.46	9.83	18.30	0.12 ± 0.03
	9	34.65	3.32	<0.001	85.99	59.96–104.82	8.77		-0.12 ± 0.03
Sperm head morphology index	4	67.84	6.82	<0.001	154.51	149.56–155.46	12.93	45.35	0.35 ± 0.08
	8	45.05	5.08	<0.001	113.45	95.68–129.09	9.36		-0.4 ± 0.08
	9	34.65	9.33	<0.001	85.99	85.99–85.99	18.41		-0.5 ± 0.08
	15	22.74	5.72	<0.001	78.25	76.5–78.25	10.65		0.42 ± 0.08
	4:9	NA	3.95	<0.001	NA	NA	7.14	NA	0.70 ± 0.16

QTL identified using nonparametric interval mapping were not assessed using multiple QTL mapping.

^a The percent of the phenotypic variance explained by each QTL.

^b The percent of the phenotypic variance explained by all terms (e.g., all QTL) in the model.

^c The difference between the phenotype averages of the *musculus*^{PWK} and *musculus*^{CZII} alleles. A negative effect indicates the *musculus*^{CZII} allele lowers the reproductive phenotype value.

^d Square-root transformed sperm count (1×10^6).

(Chrs 1, 2, 4, 7, 8, 9, and 15). We found no evidence of epistatic interactions (Table S1), although sample sizes were likely too small to detect such effects. Multiple QTL models supported several loci contributing to sperm count and abnormal sperm head morphology, consistent with our single QTL results (Table 3). Neither Chr Y origin nor genotyped *Prdm9* alleles were associated with hybrid sterility phenotypes (Table S2).

Hybrid sterility QTL colocalized with TRD on Chr 4

Sterility phenotypes associated with the *musculus*^{PWK} allele on Chr 4 colocalized with a large region (46.91:153.39 Mb) that had a deficit of *musculus*^{PWK} alleles at 50 consecutive markers (expected allelic ratio: 50:50, median observed 39.5:60.5, χ^2 test, $P \leq 0.05$; Figure 2, C and D). The most extreme TRD was observed at 116.01:151.14 Mb (median observed 38.7:61.3, χ^2 test, $P \leq 0.001$) and was also observed when crosses were parsed by sire (*musculus*^{PWK} × *CZII* sire, $N = 75$, 33.3:66.7; *musculus*^{CZII} × *PWK* sire $N = 75$, 44.3:55.7). Sex ratios were normal in these crosses (females:males 51:49, χ^2 test, $P = 0.701$). The Chr 4 region showing TRD overlapped with QTL for lower sperm count (± 1.5 LOD interval 90.72–155.46) and more abnormal sperm head and tail morphology (± 1.5 LOD interval 4.17–180.22) in males with the *musculus*^{PWK} allele. This could be due to chance given that the ± 1.5 LOD intervals for all sterility QTL encompassed 19.1% (275.59 cM) of the total genome, although sterility QTL associated with *musculus*^{PWK} alleles encompassed only 5.5% of the genome (79.16 cM total).

Chr 4 sterility and TRD loci showed unusual patterns of introgression

The distal region of Chr 4 showing TRD contained an unusually high density of SNPs between *musculus*^{CZII} and *musculus*^{PWK} (hypergeometric test, $P < 0.001$). Previous work has shown appreciable subspecific introgression into *musculus*^{PWK}, including a large tract of *M. m. domesticus* introgression on the distal portion of Chr 4 (Yang *et al.* 2011).

Consistent with this, we found considerable genome-wide introgression between *musculus*^{PWK} and *M. m. domesticus* (median *D*-statistic of 0.253, Figure 3A). Across most chromosomes, *D*-statistic estimates were similar regardless of which *M. m. domesticus* strain was used. On Chr 4 we detected introgression between *M. m. domesticus* (*domesticus*^{WSB}, *domesticus*^{LEW}) and *musculus*^{PWK}, but not between *domesticus*^{C57} and *musculus*^{PWK}. Discordance in the *D*-statistic among *M. m. domesticus* strains was localized to a 20 Mb region on the distal end of Chr 4 (130–150 Mb), coincident with the *musculus*^{PWK} sterility QTL and the region with the strongest TRD (Figure 3B). For simplicity, we will refer to this narrower region as the Chr 4 TRD locus.

We then contrasted patterns of divergence outside and inside of the Chr 4 TRD locus using other *M. m. musculus* inbred strains and wild house mice (Yang *et al.* 2011; Harr *et al.* 2016). Wild mice strongly clustered by subspecies both outside and inside of the TRD locus (Figure 4A). In contrast, some *M. m. musculus* wild-derived strains (PWK and PWD) clustered with *M. m. domesticus* at the TRD region while classic laboratory strains (primarily *M. m. domesticus* in origin) showed a mosaic of subspecific origins within the Chr 4 TRD locus (Figure 4B). We then estimated gametic disequilibrium between Chr 4 (130–150 Mb) and 1313 autosomal and Y-linked SNPs to test for other genomic regions that may be associated with the Chr 4 TRD locus. Overall, gametic disequilibrium was low (r^2 : median 0.014, maximum 0.645), and similar to prior estimates (Payseur and Hoekstra 2005). Seven SNPs showed elevated r^2 (Table S3), but we did not find any SNPs that had high r^2 values across the Chr 4 TRD haplotype. There was no association between Chr 4 and Chr Y, which has either a *M. m. musculus* or *M. m. domesticus* origin in the classic strains (Bishop *et al.* 1985).

To evaluate the deeper evolutionary origin of the Chr 4 TRD locus, we estimated the phylogenies across 10 species of *Mus* for Chr 3 (a similar sized chromosome with limited introgression relative to other chromosomes and no TRD) and Chr 4 regions outside and inside the TRD locus. Concatenated trees for Chr 3 and non-TRD Chr 4 (Figure S2) were

801
802
803
804
805
806
807
808
809
810
811
812
813
814
815
816
817
818
819
820
821
822
823
824
825
826
827
828
829
830
831
832
833
834
835
836
837
838
839
840
841
842
843
844
845
846
847
848
849
850
851
852
853
854
855
856

857
858
859
860
861
862
863
864
865
866
867
868
869
870
871
872
873
874
875
876
877
878
879
880
881
882
883
884
885
886
887
888
889
890
891
892
893
894
895
896
897
898
899
900
901
902
903
904
905
906
907
908
909
910
911
912

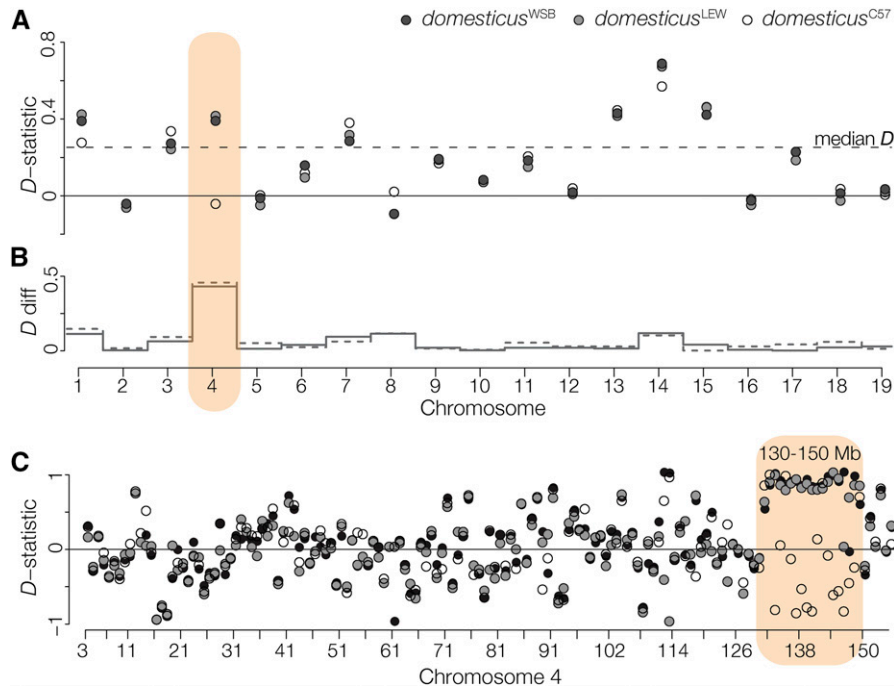


Figure 3 Introgression between *M. m. musculus* and *M. m. domesticus*. (A) *D*-statistics, calculated for each chromosome, testing for introgression between *musculus*^{CZII} or *musculus*^{PWK} and *M. m. domesticus*. The median *D*-statistic across all *M. m. domesticus* comparisons is represented by the dashed line. Patterns on Chr 4 vary depending on the strain of *M. m. domesticus*. (B) The absolute difference in the *D*-statistic using *domesticus*^{WSB} (solid gray line) or *domesticus*^{LEW} (dashed gray line) compared to *domesticus*^{C57}. (C) *D*-statistic calculated over 1 Mb nonoverlapping windows localizes discordant introgression to a 20 Mb window on the distal end of Chr 4.

913
914
915
916
917
918
919
920
921
922
923
924
925
926
927
928
929
930
931
932
933
934
935
936
937
938
939
940
941
942
943
944
945
946
947
948
949
950
951
952
953
954
955
956
957
958
959
960
961
962
963
964
965
966
967
968

consistent with previous species tree estimates (Sarver *et al.* 2017). In contrast, trees from the Chr 4 TRD locus showed reciprocal swapping of *M. m. musculus* and *M. m. domesticus* strains, with *musculus*^{PWK} closest to *domesticus*^{WSB} and *musculus*^{CZII} closest to *domesticus*^{C57}. These conflicting patterns were most apparent using a gene-tree approach to characterize patterns of fine-scale topological discordance across Chr 4 (Figure 4C). We found no other *Mus* lineages with variant topologies for the Chr 4 TRD region.

TRD was restricted to hybrid crosses and was not associated with sperm motility

Male meiotic drivers often operate through various mechanisms of sperm impairment (Lindholm *et al.* 2016). In the classic house mouse *t* complex drive system, heterozygous males show a higher frequency in motile sperm of the sperm killing Chr 17 *t* haplotype (Lyon 2003). We used whole genome sequencing of sperm pools to test if the higher frequency of the *musculus*^{CZII} Chr 4 TRD haplotype in the offspring of the F1 hybrid test cross reflected motility differences in the sperm of the *M. m. musculus* (*musculus*^{PWK} × *musculus*^{CZII}) sires. We generated between 40 and 64 million uniquely mapped reads (MQ ≥ 56) from the motile and immotile sperm fractions of four F1 *M. m. musculus* males. An average of 7 million reads per sample spanned at least one diagnostic SNP. We parsed reads into 5463 overlapping 1 Mb windows and analyzed an average of 4777 windows with ≥100 mapped reads and ≥1 diagnostic SNP (QUAL ≥ 24). No window showed significant skew between motile and immotile sperm pools in any male. In an additional experiment, we confirmed that the Percoll method was effective in separating motile from immotile sperm (Figure S3).

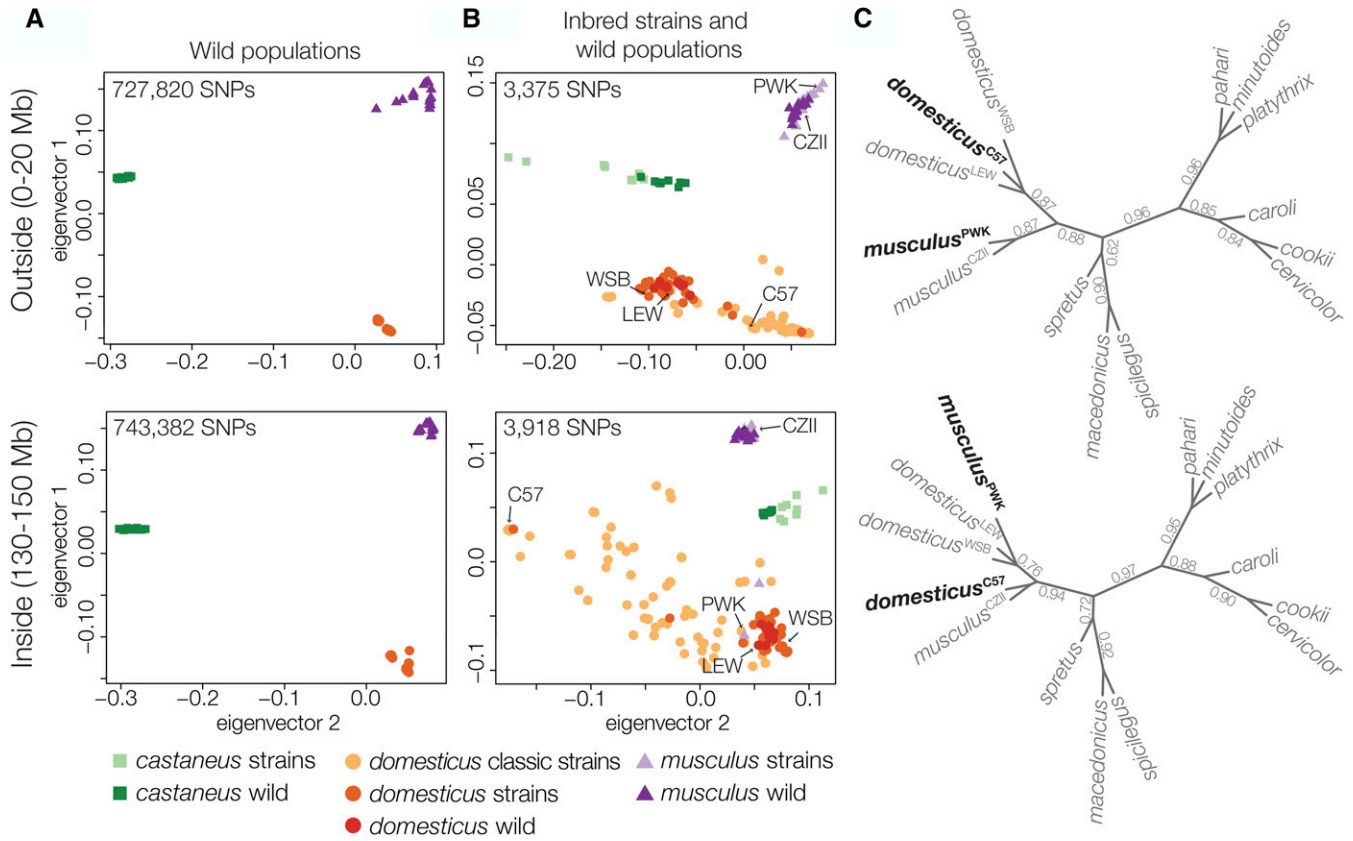
Our sequencing experiment demonstrated that Chr 4 TRD is likely not related to sperm motility and therefore must reflect genotypic differences in sperm competitive interactions (including female choice), fertilization ability, or postzygotic development. To localize the timing of distortion, we crossed the same *M. m. musculus* sire genotype (*musculus*^{PWK} × *musculus*^{CZII}) to *musculus*^{PWK} females to generate 602 backcross offspring (319 female and 283 male) from 133 litters. We generated ddRADseq libraries for 312 backcross mice. After removing individuals with low coverage, we retained 303 mice that had between 156,791 and 3,315,067 uniquely mapped reads (median of 664,627 per mouse, total of 232,515,877 single reads) and we constructed a genetic map using 358 high-quality SNPs. We found no evidence of TRD on Chr 4 (expected allelic ratio, 50:50; median observed, 50:50) and this pattern held when parsed by sire, sex, or sire and sex. To confirm these results, we genotyped an additional 193 backcross mice using microsatellite markers spanning Chr 4 and still found no evidence of TRD (*N* = 496 mice; Table 4). Thus, Chr 4 TRD between *musculus*^{CZII} and *musculus*^{PWK} alleles was only observed in crosses involving *domesticus*^{WSB} females (Figure 5A).

Discussion

Polymorphic HMS has a polygenic basis in house mice

Individuals often vary in the degree that they are reproductively isolated from other lineages, but the genetic basis and evolutionary origin of such variation remains poorly understood. In house mice, there is considerable variability in the strength of F1 HMS in crosses using different inbred strains or wild isolates of *M. m. musculus* and *M. m. domesticus* (Britton-

969
970
971
972
973
974
975
976
977
978
979
980
981
982
983
984
985
986
987
988
989
990
991
992
993
994
995
996
997
998
999
1000
1001
1002
1003
1004
1005
1006
1007
1008
1009
1010
1011
1012
1013
1014
1015
1016
1017
1018
1019
1020
1021
1022
1023
1024



1025
1026
1027
1028
1029
1030
1031
1032
1033
1034
1035
1036
1037
1038
1039
1040
1041
1042
1043
1044
1045
1046
1047
1048
1049
1050
1051
1052
1053
1054
1055
1056
1057
1058
1059
1060
1061
1062
1063
1064
1065
1066
1067
1068
1069
1070
1071
1072
1073
1074
1075
1076
1077
1078
1079
1080

Figure 4 Patterns of discordance outside and inside the Chr 4 TRD locus. (A) Principal components analysis of SNPs from whole genome sequencing of eight wild populations of *M. m. musculus*, *M. m. domesticus*, and *M. m. castaneus* (Harr et al. 2016) and (B) the Mouse Diversity Array for wild mice (dark colors) and classic laboratory and wild-derived strains of mice (light colors) (Yang et al. 2011). There was strong clustering of SNPs in wild populations, both outside and inside the TRD region, but the classic strains showed mixed SNP clustering. (C) Unrooted species trees estimated across 100 kbp windows outside and inside the Chr 4 TRD locus. Branches are annotated with their local quartet scores.

Davidian et al. 2005; Vyskočilová et al. 2005; Good et al. 2008b; Bhattacharyya et al. 2014). One simple interpretation of these results is that there are one or a few common incompatibilities that are polymorphic within *M. m. musculus* and/or *M. m. domesticus* populations. Consistent with this, the only HMS gene yet identified in mammals, *Prdm9*, appears to be polymorphic for sterile and fertile alleles within both *M. m. musculus* and *M. m. domesticus* (Forejt and Ivanyi 1974; Vyskočilová et al. 2009; Flachs et al. 2012). While the evolutionary origin and extent of *Prdm9*-linked HMS variation remains unclear in natural populations, our results reveal that there is likely to be considerable polymorphism at other HMS loci.

We identified five autosomal regions that contributed to variation in HMS in crosses between *M. m. domesticus* females and *M. m. musculus* males, despite sampling just two wild-derived inbred strains of *M. m. musculus* (Figure 2). F1 hybrid males from crosses between female *M. m. domesticus* and *musculus*^{PWK} yield only weak sterility phenotypes, while crosses involving *musculus*^{CZII} are more severely sterile in both directions of the cross (Table 1; Good et al. 2008b). Surprisingly, considerable variation exists beneath this seemingly simple F1 architecture. Sterility loci were associated

with both strains; sterility alleles on Chrs 2, 8, and 9 derived from *musculus*^{CZII}, while *musculus*^{PWK} sterility variants were mapped to Chr 4 and Chr 15.

F1 HMS variability has been observed in other *M. m. musculus* strains (Piálek et al. 2008; Bhattacharyya et al. 2014) and in wild *M. m. musculus* isolated from eastern Czechia (Good et al. 2008b). Thus, the polymorphic HMS that we document here may be relatively widespread within *M. m. musculus* (Vyskočilová et al. 2005; Good et al. 2008b; Bhattacharyya et al. 2014). Consistent with this, there was some overlap between the HMS loci we identified and HMS QTL from other studies (Figure 2A). Bhattacharyya et al. (2014) used a similar experimental design between *domesticus*^{C57} females and *M. m. musculus* interstrain males (PWD and STUS) to map polymorphic hybrid sterility to Chr 9 (sperm count). Sterility loci were identified on Chr 4 (epididymis weight) in recombinant inbred lines derived from all three *M. m. musculus* subspecies (Shorter et al. 2017), Chr 4 (testis weight) and Chr 15 (abnormal sperm morphology) were identified in F2 crosses between *domesticus*^{WSB} and *M. m. musculus* PWD (White et al. 2011; Turner et al. 2014), and Chr 2 and Chr 9 were associated with low testis weights in wild-caught hybrid mice (Turner and Harr 2014). However,

1081 **Table 4 Summary of genotype frequencies in *M. m. musculus***
 1082 **backcross**

	Crosses	AA	AB	Total	%AB	P-value
1084	Region 1					
1085	140,089,156–					
1086	141,037,913 bp					
1087	<i>musculus</i> ^{CZII} × <i>PWK</i> sire	100	93	195	47.7	0.614
1088	females	54	50	106	47.2	0.695
1089	males	46	43	89	48.3	0.75
1090	<i>musculus</i> ^{PWK} × <i>CZII</i> sire	144	157	301	52.2	0.454
1091	females	77	83	160	51.9	0.635
1092	males	67	74	141	52.5	0.556
1093	Total	244	250	496	50.4	0.787
1094	Region 2					
1095	148,602,050–					
1096	151,609,913 bp					
1097	<i>musculus</i> ^{CZII} × <i>PWK</i> sire	97	97	195	49.7	1
1098	females	53	53	106	50	1
1099	males	44	44	89	49.4	1
1100	<i>musculus</i> ^{PWK} × <i>CZII</i> sire	138	162	301	53.8	0.166
1101	females	73	86	160	53.8	0.303
1102	males	65	76	141	53.9	0.354
1103	total	235	259	496	52.2	0.28

1096 To test for TRD within *M. m. musculus*, female *musculus*^{PWK} were crossed to re-
 1097 ciprocal interstrain F1s between *musculus*^{CZII} and *musculus*^{PWK}. Offspring were
 1098 genotyped for two regions inside the introgressed TRD on Chr 4.

1100 these studies also found sterility QTL on Chrs 1, 2, 3, 5, 6, 10,
 1101 12, 13, 14, 17, and 18, which implies that nearly every auto-
 1102 some is linked to some form of HMS. The emerging picture is
 1103 of an increasingly complex genetic basis to HMS that depends
 1104 strongly on genotype. Indeed, multiple polymorphic hybrid
 1105 sterility factors would account for the variable fertility of
 1106 multigeneration hybrids from the center of the hybrid zone
 1107 (Turner *et al.* 2012). Inbred line crosses remain one of the
 1108 most powerful and quantitative tools for the genetic dissec-
 1109 tion of hybrid incompatibilities. However, the common as-
 1110 sumption that most incompatibilities reflect fixed differences
 1111 between lineages appears increasingly tenuous, especially dur-
 1112 ing the early stages of speciation. This realization has the
 1113 potential to broadly impact important issues in speciation ge-
 1114 netics. In addition to the need to incorporate population-level
 1115 sampling into the design of mapping studies on the genetics of
 1116 speciation, many theoretical predications on the accumulation
 1117 of reproductive isolation are based on epistatic models that
 1118 treat interacting hybrid incompatibilities as fixed within species
 1119 (*e.g.*, Orr and Turelli 2001; Wang *et al.* 2013; Lindtke and
 1120 Buerkle 2015).

1121 **The causes of polymorphic reproductive isolation**

1123 Several incompatibilities are polymorphic in house mice, but
 1124 the origins of these variants are unclear. One possible source is
 1125 introgression at previously fixed incompatibilities. Alleles
 1126 contributing to hybrid incompatibilities should have restricted
 1127 introgression relative to the rest of the genome. Indeed, the
 1128 identification of loci showing restricted gene flow across
 1129 hybrid zones is a powerful approach to identifying alleles that
 1130 contribute to reproductive barriers (Barton and Hewitt 1985;
 1131 Harrison 1990; Payseur 2010). However, gene flow and re-
 1132 combination within a hybrid zone can quickly break down
 1133 epistatic interactions among BDIMs (Virdee and Hewitt
 1134 1994; Shuker *et al.* 2005; Bank *et al.* 2012; Lindtke and Buer-
 1135 kle 2015), which could in turn result in polymorphic incom-

1136

1137 patibilities. The house mouse hybrid zone is wide relative to
 1138 the dispersal distances of mice. As a result, pure *M. m. domesticus*
 1139 and *M. m. musculus* rarely come into contact and few F1 mice
 1140 are found in the hybrid zone. The zone is primarily composed
 1141 of complex, multigeneration hybrids that show extensive var-
 1142 iation in the severity of HMS (Janoušek *et al.* 2012; Turner
 1143 *et al.* 2012; Turner and Harr 2014), which likely reflects the
 1144 partial breakdown of epistatic reproductive barriers.

1145 Several of the common wild-derived strains show appreci-
 1146 able introgression between subspecies of *M. m. musculus*,
 1147 including *musculus*^{PWK} (Yang *et al.* 2011; Sarver *et al.* 2017).
 1148 Four of our polymorphic HMS regions did not colocalize with
 1149 strong signatures of introgression (results not shown), al-
 1150 though gene flow cannot be ruled out at our current mapping
 1151 resolution. At least one HMS region (Chr 4) did coincide with
 1152 introgression into *musculus*^{PWK} (Figure 3), but not necessari-
 1153 ally in the direction predicted if HMS polymorphism reflects
 1154 the partial erosion of reproductive barriers. Hybrid sterility
 1155 QTL on Chr 4 contributed to low sperm counts and abnormal
 1156 sperm morphology in males carrying the *musculus*^{PWK} allele
 1157 (Figure 2A). Coincident with the Chr 4 HMS QTL, an ~20 Mb
 1158 *M. m. domesticus* haplotype (represented here by *domesti-*
 1159 *cus*^{WSB} and *domesticus*^{LEW}) was introgressed into *muscu-*
 1160 *lus*^{PWK}, while a *M. m. musculus* haplotype (represented by
 1161 *musculus*^{CZII}) appears introgressed into *domesticus*^{C57} (Figure
 1162 3) and some other classic strains (Figure 4, Yang *et al.* 2011).
 1163 At least two *M. m. musculus* strains (PWK and PWD) derived
 1164 from different localities carry introgressed *M. m. domesticus*
 1165 haplotypes. In other words, a *M. m. domesticus*-derived hy-
 1166 brid sterility locus has introgressed into at least two independ-
 1167 ent *M. m. musculus* strains. Transmission of the same
 1168 introgressed *musculus*^{PWK} allele was also underrepresented
 1169 in our hybrid test cross (Figure 2C). Thus, the distal end of
 1170 Chr 4 shows a propensity to reciprocally introgress between
 1171 *M. m. musculus* and *M. m. domesticus* genomes despite asym-
 1172 metric TRD and detrimental effects on hybrid fertility.

1173 How can recurrent reciprocal introgression be reconciled
 1174 with the evolution of HMS and TRD in the same genomic
 1175 region? Non-Mendelian segregation is common in divergent
 1176 crosses and can reflect differences in gamete production,
 1177 fertilization, and zygote survival (Lindholm *et al.* 2016).
 1178 For example, sexual selection can lead to TRD when gametes
 1179 carrying different alleles have contrasting fertilization abil-
 1180 ities due to male gamete competition or cryptic female choice
 1181 (*e.g.*, Fishman *et al.* 2008). We did not observe TRD in our
 1182 independent *M. m. musculus* backcross or distal Chr 4 intro-
 1183 gression in wild mice, arguing against simple competitive
 1184 advantage of the *musculus*^{CZII} haplotype. In divergent
 1185 crosses, TRD is often caused by biased transmission of selfish
 1186 genetic elements (*i.e.*, meiotic drive or segregation distortion;
 1187 McDermott and Noor 2010; Lindholm *et al.* 2016) as found,
 1188 for example, at the *R2d2* locus in house mice (Didion *et al.*
 1189 2015, 2016). Drive elements generate intragenomic conflict,
 1190 which should drive strong counter selection for unlinked
 1191 drive suppressors. Drive systems coevolve independently in
 1192 isolated populations, which can lead to sterility when drivers

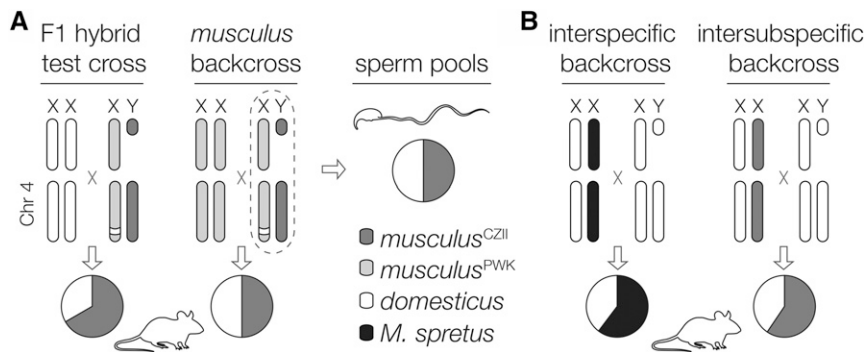


Figure 5 Summary of Chr 4 TRD. (A) The *musculus*^{PWK} haplotype on the distal portion of Chr 4, which is derived from *M. m. domesticus*, was undertransmitted in the offspring of crosses involving *M. m. domesticus* females and *M. m. musculus* males, but not in *M. m. musculus* backcrosses or the sperm of *M. m. musculus* males. (B) Two other crosses have reported reduced transmission of the distal portion of Chr 4 derived from *M. m. domesticus*, but through females. The first was an interspecific cross between F1 females (*M. m. domesticus* C57BL/6J \times *M. spretus*) and *M. m. domesticus* C57BL/6J males (TRD \sim 73 Mb to end of Chr 4; Ceci *et al.* 1989), and the second was an interspecific cross between interstrain F1 females (*M. m. domesticus* C57BL/KsJ \times *musculus*^{CZII}) and *M. m. domesticus* C57BL/KsJ males (TRD \sim 107–138 Mb; Fiedorek and Kay 1994).

and suppressers are uncoupled in hybrid genomes (Frank 1991; Hurst and Pomiankowski 1991). Male meiotic drivers often act by impairing the development or fertilization capacity of nondriving sperm (Lindholm *et al.* 2016). We tested this scenario directly and found no TRD between motile and immotile sperm of *musculus*^{PWK} \times *CZII* males. More broadly, TRD on the distal region of Chr 4 has also been reported in two other divergent crosses: TRD favoring the distal Chr 4 *M. spretus* allele in crosses between *domesticus*^{C57} \times *M. spretus* F1 females and *domesticus*^{C57} males (Ceci *et al.* 1989), and TRD again favoring the *musculus*^{CZII} distal Chr 4 allele in crosses between *domesticus*^{C57BL/KsJ} males and *domesticus*^{C57BL/KsJ} \times *musculus*^{CZII} F1 females (Fiedorek and Kay 1994). Importantly, both crosses reveal reduced transmission of the distal portion of Chr 4 derived from *M. m. domesticus* through female gametogenesis (Figure 5B). If these patterns reflect a common mechanism, then Chr 4 TRD must act independent of male-specific mechanisms.

Collectively, these results suggest that Chr 4 TRD and introgression are both a consequence of incompatibilities that reduce hybrid embryo viability (postzygotic inviability). In principle, TRD could occur because of a negative interaction between egg (or female reproductive tract) and sperm resulting in reduced fertilization (postmating prezygotic barriers) (Nadeau 2017), although incompatible egg–sperm interactions are often asymmetric (*i.e.*, depend on the parent of origin of gametes; Larson *et al.* 2012). Chr 4 TRD occurs in crosses involving both male and female *M. m. domesticus*, with consistent bias against the Chr 4 *M. m. domesticus* allele when backcrossed to *M. m. domesticus* (Figure 5). The simplest explanation for this pattern is a two locus BDMI involving a recessive Chr 4 incompatibility derived in the *M. m. domesticus* lineage. It remains unclear why TRD driven by hybrid inviability in crosses involving *M. m. domesticus* colocalizes with HMS QTL that manifests in the F1 offspring. It is possible that early-acting hybrid inviability leads to the pleiotropic impairment of other reproductive traits. Alternatively, this region may harbor multiple incompatibilities, which ap-

pears to be the case for TRD of polymorphic hybrid incompatibilities in monkeyflowers (Kerwin and Sweigart 2017).

Under an inviability model, introgression at the Chr 4 TRD locus in various classic and wild-derived inbred strains (*i.e.*, *musculus*^{PWK}, *PWD*) would reflect different outcomes of selection against particular incompatible allelic pairings. Such epistatic selection should generate linkage disequilibrium between distal Chr 4 and other genomic regions within hybrid genomes. Although our initial scan of genotypes from 76 classic laboratory strains failed to detect these associations (Table S3), multiple genome-wide studies have revealed that selection against other deleterious allelic combinations has shaped the mosaic composition of introgressed laboratory strains (Payseur and Hoekstra 2005; Petkov *et al.* 2005) and the *M. m. domesticus*–*M. m. musculus* hybrid zone (Turner *et al.* 2012; Turner and Harr 2014). There has been considerable effort to resolve the extent to which various classic and common wild-derived laboratory strains are introgressed, with an emphasis on overall strain genetic purity (Yang *et al.* 2011; Didion and Pardo-Manuel de Villena 2012). While overall admixture proportions are of some relevance, our results suggest that specific genome-wide patterns of introgression may be strongly shaped by selection with the unexpected result that selection against epistatic BDIMs may facilitate introgression at underlying loci. These results underscore the intricacies of nascent species boundaries during the early stages of speciation when reproductive isolation remains incomplete and genetically variable.

Acknowledgments

We thank Kathleen Tsung, Joseph Dysthe, Brent Young, Nick Schultz, Selene Tyndale, and Charlie Nicolet for assistance with data collection and analysis. We also thank members of the Good laboratory; Ryan Bracewell, Lila Fishman, David Aylor, Bret Payseur, Michael Nachman, Peter Ellis, and two anonymous reviewers for helpful feedback; the Vincent J. Coates Genomics Sequencing Laboratory at the University of California Berkeley, sup-

- ported by the National Institutes of Health S10 instrumentation grants S1ORR029668 and S1ORR027303; and the University of Montana Genomics Core, supported by a grant from the M.J. Murdock Charitable Trust. This research was supported by the Eunice Kennedy Shriver National Institute of Child Health and Human Development of the National Institutes of Health (R01-HD073439 and R01-HD094787 to J.M.G.), the National Institute of General Medical Sciences (R01-GM098536 to M.D.D.), and the National Science Foundation (1146525 to M.D.D.).
- Author contributions: J.M.G. conceived the study. J.M.G., E.L.L., and M.D.D. designed the experiments. E.L.L., D.V., C.C., V.S., E.N., and L.P.P. performed experiments and collected data. E.L.L., D.V., B.A.J.S., S.K., L.P.P., M.D.K., and M.D.D. analyzed data. E.L.L. and J.M.G. wrote the manuscript with feedback from the authors.
- ### Literature Cited
- Baker, C. L., S. Kajita, M. Walker, R. L. Saxl, N. Raghupathy *et al.*, 2015 PRDM9 drives evolutionary erosion of hotspots in *Mus musculus* through haplotype-specific initiation of meiotic recombination. *PLoS Genet.* 11: e1004916. <https://doi.org/10.1371/journal.pgen.1004916>
- Bank, C., R. Bürger, and J. Hermisson, 2012 The limits to parapatric speciation: dobzhansky–Muller incompatibilities in a continent–island model. *Genetics* 191: 845–863. <https://doi.org/10.1534/genetics.111.137513>
- Barton, N. H., and G. M. Hewitt, 1985 Analysis of hybrid zones. *Annu. Rev. Ecol. Syst.* 16: 113–148. <https://doi.org/10.1146/annurev.es.16.110185.000553>
- Bateson, W., 1909 Heredity and variation in modern lights, pp. 85–101 in *Darwin and Modern Science*, edited by A. C. Seward. Cambridge University Press, Cambridge, UK.
- Benjamini, Y., and Y. Hochberg, 1995 Controlling the false discovery rate: a practical and powerful approach to multiple testing. *J. R. Stat. Soc.* 57: 289–300.
- Bhattacharyya, T., S. Gregorova, O. Mihola, M. Anger, J. Sebestova *et al.*, 2013 Mechanistic basis of infertility of mouse intersub-specific hybrids. *Proc. Natl. Acad. Sci. USA* 110: E468–E477. <https://doi.org/10.1073/pnas.1219126110>
- Bhattacharyya, T., R. Reifova, S. Gregorova, P. Simecek, V. Gergelits *et al.*, 2014 X chromosome control of meiotic chromosome synapsis in mouse inter-subspecific hybrids. *PLoS Genet.* 10: e1004088. <https://doi.org/10.1371/journal.pgen.1004088>
- Bishop, C. E., P. Boursot, B. Baron, F. Bonhomme, and D. Hatat, 1985 Most classical *Mus musculus domesticus* laboratory mouse strains carry a *Mus musculus musculus* Y chromosome. *Nature* 315: 70–72. <https://doi.org/10.1038/315070a0>
- Britton-Davidian, J., F. Fel-Clair, J. Lopez, P. Alibert, and P. Boursot, 2005 Postzygotic isolation between the two European subspecies of the house mouse: estimates from fertility patterns in wild and laboratory-bred hybrids. *Biol. J. Linn. Soc. Lond.* 84: 379–393. <https://doi.org/10.1111/j.1095-8312.2005.00441.x>
- Broman, K. W., H. Wu, S. Sen, and G. A. Churchill, 2003 R/qtl: QTL mapping in experimental crosses. *Bioinformatics* 19: 889–890. <https://doi.org/10.1093/bioinformatics/btg112>
- Campbell, P., and M. W. Nachman, 2014 X-Y interactions underlie sperm head abnormality in hybrid male house mice. *Genetics* 196: 1231–1240. <https://doi.org/10.1534/genetics.114.161703>
- Campbell, P., J. M. Good, and M. W. Nachman, 2013 Meiotic sex chromosome inactivation is disrupted in sterile hybrid male house mice. *Genetics* 193: 819–828. <https://doi.org/10.1534/genetics.112.148635>
- Carter, T. C., and D. S. Falconer, 1951 Stocks for detecting linkage in the mouse, and the theory of their design. *J. Genet.* 50: 307–323. <https://doi.org/10.1007/BF02996226>
- Case, A. L., F. R. Finseth, C. M. Barr, and L. Fishman, 2016 Selfish evolution of cytonuclear hybrid incompatibility in *Mimulus*. *Proc. Biol. Sci.* 283: 20161493–20161499. <https://doi.org/10.1098/rspb.2016.1493>
- Ceci, J. D., L. D. Siracusa, N. A. Jenkins, and N. G. Copeland, 1989 A molecular genetic linkage map of mouse chromosome 4 including the localization of several proto-oncogenes. *Genomics* 5: 699–709. [https://doi.org/10.1016/0888-7543\(89\)90111-0](https://doi.org/10.1016/0888-7543(89)90111-0)
- Chang, C. C., C. C. Chow, L. C. Tellier, S. Vattikuti, S. M. Purcell *et al.*, 2015 Second-generation PLINK: rising to the challenge of larger and richer datasets. *GigaSci* 4: 7–16. <https://doi.org/10.1186/s13742-015-0047-8>
- Christie, P., and M. R. Macnair, 1987 The distribution of postmating reproductive isolating genes in populations of the yellow monkey flower, *Mimulus guttatus*. *Evolution* 41: 571–578. <https://doi.org/10.1111/j.1558-5646.1987.tb05827.x>
- Copeland, N. G., N. A. Jenkins, D. J. Gilbert, J. T. Eppig, L. J. Maltais *et al.*, 1993 A genetic linkage map of the mouse: current applications and future prospects. *Science* 262: 57–66. <https://doi.org/10.1126/science.8211130>
- Cutter, A. D., 2012 The polymorphic prelude to Bateson-Dobzhansky-Muller incompatibilities. *Trends Ecol. Evol.* 27: 209–218. <https://doi.org/10.1016/j.tree.2011.11.004>
- Danecek, P., A. Auton, G. Abecasis, C. A. Albers, E. Banks *et al.*, 2011 The variant call format and VCFtools. *Bioinformatics* 27: 2156–2158. <https://doi.org/10.1093/bioinformatics/btr330>
- Davies, B., E. Hatton, N. Altemose, J. G. Hussin, F. Pratto *et al.*, 2016 Re-engineering the zinc fingers of PRDM9 reverses hybrid sterility in mice. *Nature* 530: 171–176. <https://doi.org/10.1038/nature16931>
- Didion, J. P., and F. Pardo-Manuel de Villena, 2012 Deconstructing *Mus gemischus*: advances in understanding ancestry, structure, and variation in the genome of the laboratory mouse. *Mamm. Genome* 24: 1–20. <https://doi.org/10.1007/s00335-012-9441-z>
- Didion, J. P., A. P. Morgan, A. M. F. Clayshulte, R. C. McMullan, L. Yadgary *et al.*, 2015 A multi-megabase copy number gain causes maternal transmission ratio distortion on mouse chromosome 2. *PLoS Genet.* 11: e1004850. <https://doi.org/10.1371/journal.pgen.1004850>
- Didion, J. P., A. P. Morgan, L. Yadgary, T. A. Bell, R. C. McMullan *et al.*, 2016 *R2d2* drives selfish sweeps in the house mouse. *Mol. Biol. Evol.* 33: 1381–1395. <https://doi.org/10.1093/molbev/msw036>
- Dobzhansky, T., 1937 *Genetics and the Origin of Species*. Columbia University Press, New York.
- Durand, E. Y., N. Patterson, D. Reich, and M. Slatkin, 2011 Testing for ancient admixture between closely related populations. *Mol. Biol. Evol.* 28: 2239–2252. <https://doi.org/10.1093/molbev/msr048>
- Fiedorek, F. T., and E. S. Kay, 1994 Mapping of PCR-based markers for mouse chromosome 4 on a backcross penetrant for the misty (m) mutation. *Mamm. Genome* 5: 479–485. <https://doi.org/10.1007/BF00369316>
- Fishman, L., J. Aagaard, and J. C. Tuthill, 2008 Toward the evolutionary genomics of gametophytic divergence: patterns of transmission ratio distortion in monkeyflower (*Mimulus*) hybrids reveal a complex genetic basis for conspecific pollen precedence. *Evolution* 62: 2958–2970. <https://doi.org/10.1111/j.1558-5646.2008.00475.x>
- Flachs, P., O. Mihola, P. Simecek, S. Gregorova, J. C. Schimenti *et al.*, 2012 Interallelic and intergenic incompatibilities of the

- 1417 *Prdm9* (Hst1) gene in mouse hybrid sterility. *PLoS Genet.* 8:
1418 e1003044. <https://doi.org/10.1371/journal.pgen.1003044>
- 1419 Flachs, P., T. Bhattacharyya, O. Mihola, J. Piálék, J. Forejt *et al.*,
1420 2014 *Prdm9* incompatibility controls oligospermia and de-
1421 layed fertility but no selfish transmission in mouse intersub-
1422 specific hybrids. *PLoS One* 9: e95806. <https://doi.org/10.1371/journal.pone.0095806>
- 1423 Forejt, J., and P. Ivanyi, 1974 Genetic studies on male sterility of
1424 hybrids between laboratory and wild mice (*Mus musculus* L.). *Genet.*
1425 *Res.* 24: 189–206. <https://doi.org/10.1017/S0016672300015214>
- 1426 Frank, S. A., 1991 Divergence of meiotic drive-suppression sys-
1427 tems as an explanation for sex-biased hybrid sterility and invi-
1428 ability. *Evolution* 45: 262–267. <https://doi.org/10.1111/j.1558-5646>
- 1429 Geraldes, A., P. Basset, K. L. Smith, and M. W. Nachman,
1430 2011 Higher differentiation among subspecies of the house
1431 mouse (*Mus musculus*) in genomic regions with low recombina-
1432 tion. *Mol. Ecol.* 20: 4722–4736. <https://doi.org/10.1111/j.1365-294X.2011.05285.x>
- 1433 Good, J. M., M. D. Dean, and M. W. Nachman, 2008a A complex
1434 genetic basis to X-linked hybrid male sterility between two spe-
1435 cies of house mice. *Genetics* 179: 2213–2228. <https://doi.org/10.1534/genetics.107.085340>
- 1436 Good, J. M., M. A. Handel, and M. W. Nachman,
1437 2008b Asymmetry and polymorphism of hybrid male sterility
1438 during the early stages of speciation in house mice. *Evolution*
1439 62: 50–65.
- 1440 Gordon, M., 1927 The genetics of a viviparous top-minnow *Plat-*
1441 *ypoecilus*; the inheritance of two kinds of melanophores. *Genetics*
1442 12: 253–283.
- 1443 Green, R. E., J. Krause, A. W. Briggs, T. Maricic, U. Stenzel *et al.*,
1444 2010 A draft sequence of the Neandertal genome. *Science*
1445 328: 710–722. <https://doi.org/10.1126/science.1188021>
- 1446 Harr, B., E. Karakoc, R. Neme, M. Teschke, C. Pfeifle *et al.*,
1447 2016 Genomic resources for wild populations of the house
1448 mouse, *Mus musculus* and its close relative *Mus spretus*. *Sci. Data*
1449 3: 160075. <https://doi.org/10.1038/sdata.2016.75>
- 1450 Harrison, R. G., 1990 Hybrid zones: windows on evolutionary
1451 process. *Oxf. Surv. Evol. Biol.* 7: 69–128.
- 1452 Hurst, L. D., and A. Pomiankowski, 1991 Causes of sex ratio bias
1453 may account for unisexual sterility in hybrids: a new explana-
1454 tion of Haldane's rule and related phenomena. *Genetics* 128:
1455 841–858.
- 1456 Janoušek, V., L. Wang, K. Luzynski, P. Dufková, M. M. Vyskočilová
1457 *et al.*, 2012 Genome-wide architecture of reproductive isola-
1458 tion in a naturally occurring hybrid zone between *Mus musculus*
1459 *musculus* and *M. m. domesticus*. *Mol. Ecol.* 21: 3032–3047.
1460 <https://doi.org/10.1111/j.1365-294X.2012.05583.x>
- 1461 Johnson, N. A., 2010 Hybrid incompatibility genes: remnants of a
1462 genomic battlefield? *Trends Genet.* 26: 317–325. <https://doi.org/10.1016/j.tig.2010.04.005>
- 1463 Keane, T. M., L. Goodstadt, P. Danecek, M. A. White, K. Wong *et al.*,
1464 2011 Mouse genomic variation and its effect on phenotypes
1465 and gene regulation. *Nature* 477: 289–294. <https://doi.org/10.1038/nature10413>
- 1466 Kerwin, R. E., and A. L. Sweigart, 2017 Mechanisms of transmis-
1467 sion ratio distortion at hybrid sterility loci within and between
1468 *Mimulus* species. *G3* 7: 3719–3730.
- 1469 Larson, E. L., G. L. Hume, J. A. Andrés, and R. G. Harrison,
1470 2012 Post-mating prezygotic barriers to gene exchange be-
1471 tween hybridizing field crickets. *J. Evol. Biol.* 25: 174–186.
1472 <https://doi.org/10.1111/j.1420-9101.2011.02415.x>
- 1473 Lindholm, A. K., K. A. Dyer, R. C. Firman, L. Fishman, W. Forstmeier
1474 *et al.*, 2016 The ecology and evolutionary dynamics of meiotic
1475 drive. *Trends Ecol. Evol.* 31: 315–326. <https://doi.org/10.1016/j.tree.2016.02.001>
- 1476 Lindtke, D., and C. A. Buerkle, 2015 The genetic architecture of
1477 hybrid incompatibilities and their effect on barriers to introgres-
1478 sion in secondary contact. *Evolution* 69: 1987–2004. <https://doi.org/10.1111/evo.12725>
- 1479 Lohse, M., A. M. Bolger, A. Nagel, A. R. Fernie, J. E. Lunn *et al.*,
1480 2012 RobiNA: a user-friendly, integrated software solution for
1481 RNA-Seq-based transcriptomics. *Nucleic Acids Res.* 40: W622–
1482 W627. <https://doi.org/10.1093/nar/gks540>
- 1483 Lyon, M. F., 2003 Transmission ratio distortion in mice. *Annu.*
1484 *Rev. Genet.* 37: 393–408. <https://doi.org/10.1146/annurev.genet.37.110801.143030>
- 1485 Maheshwari, S., and D. A. Barbash, 2011 The genetics of hybrid
1486 incompatibilities. *Annu. Rev. Genet.* 45: 331–355. <https://doi.org/10.1146/annurev-genet-110410-132514>
- 1487 Matute, D. R., J. Gavin-Smyth, and G. Liu, 2014 Variable post-
1488 zygotic isolation in *Drosophila melanogaster*/*D. simulans* hy-
1489 brids. *J. Evol. Biol.* 27: 1691–1705. <https://doi.org/10.1111/jeb.12422>
- 1490 McDermott, S. R., and M. A. F. Noor, 2010 The role of meiotic
1491 drive in hybrid male sterility. *Philos. Trans. R. Soc. Lond. B Biol.*
1492 *Sci.* 365: 1265–1272. <https://doi.org/10.1098/rstb.2009.0264>
- 1493 McKenna, A., M. Hanna, E. Banks, A. Sivachenko, K. Cibulskis *et al.*,
1494 2010 The genome analysis toolkit: a mapReduce framework
1495 for analyzing next-generation DNA sequencing data. *Genome*
1496 *Res.* 20: 1297–1303. <https://doi.org/10.1101/gr.107524.110>
- 1497 Mihola, O., Z. Trachtulec, C. Vlcek, J. C. Schimenti, and J. Forejt,
1498 2009 A mouse speciation gene encodes a meiotic histone H3
1499 methyltransferase. *Science* 323: 373–375. <https://doi.org/10.1126/science.1163601>
- 1500 Mirarab, S., and T. Warnow, 2015 ASTRAL-II: coalescent-based
1501 species tree estimation with many hundreds of taxa and thou-
1502 sands of genes. *Bioinformatics* 31: i44–i52. <https://doi.org/10.1093/bioinformatics/btv234>
- 1503 Muller, H. J., 1942 Isolating mechanisms, evolution and temper-
1504 ature. *Biol. Symp.* 6: 71–125.
- 1505 Nadeau, J. H., 1997 Do gametes woo? Evidence for their nonran-
1506 dom union at fertilization. *Genetics* 207: 369–387.
- 1507 Ng, F. L., D. Y. Liu, and H. G. Baker, 1992 Comparison of
1508 Percoll, mini-Percoll and swim-up methods for sperm prepara-
1509 tion from abnormal semen samples. *Hum. Reprod.* 7: 261–266.
1510 <https://doi.org/10.1093/oxfordjournals.humrep.a137628>
- 1511 Odet, F., W. Pan, T. A. Bell, S. G. Goodson, A. M. Stevans *et al.*,
1512 2015 The founder strains of the collaborative cross express a
1513 complex combination of advantageous and deleterious traits for
1514 male reproduction. *G3* (Bethesda) 5: 2671–2683. <https://doi.org/10.1534/g3.115.020172>
- 1515 Oka, A., A. Mita, N. Sakurai-Yamatani, H. Yamamoto, N. Takagi
1516 *et al.*, 2004 Hybrid breakdown caused by substitution of the
1517 X chromosome between two mouse subspecies. *Genetics* 166:
1518 913–924. <https://doi.org/10.1534/genetics.166.2.913>
- 1519 Orr, A. H., and M. Turelli, 2001 The evolution of postzygotic iso-
1520 lation: accumulating Dobzhansky-Muller incompatibilities. *Evolution*
1521 55: 1085–1094. <https://doi.org/10.1111/j.0014-3820.2001.tb00628.x>
- 1522 Patterson, J. T., and W. S. Stone, 1952 *Evolution in the Genus Drosophila*. The Macmillan Company, New York.
- 1523 Payseur, B. A., 2010 Using differential introgression in hybrid
1524 zones to identify genomic regions involved in speciation. *Mol.*
1525 *Ecol. Resour.* 10: 806–820. <https://doi.org/10.1111/j.1755-0998.2010.02883.x>
- 1526 Payseur, B. A., and H. E. Hoekstra, 2005 Signatures of reproduc-
1527 tive isolation in patterns of single nucleotide diversity across
1528

- 1529 inbred strains of mice. *Genetics* 171: 1905–1916. <https://doi.org/10.1534/genetics.105.046193>
- 1530 Pease, J. B., and M. W. Hahn, 2015 Detection and polarization of
- 1531 introgression in a five-taxon phylogeny. *Syst. Biol.* 64: 651–662.
- 1532 <https://doi.org/10.1093/sysbio/syv023>
- 1533 Peterson, B. K., J. N. Weber, E. H. Kay, H. S. Fisher, and H. E.
- 1534 Hoekstra, 2012 Double digest RADseq: an inexpensive method
- 1535 for de novo SNP discovery and genotyping in model and non-model
- 1536 species. *PLoS One* 7: e37135. <https://doi.org/10.1371/journal.pone.0037135>
- 1537 Petkov, P. M., J. H. Graber, G. A. Churchill, K. DiPetrillo, B. L. King
- 1538 *et al.*, 2005 Evidence of a large-scale functional organization
- 1539 of mammalian chromosomes. *PLoS Genet.* 1: e33. <https://doi.org/10.1371/journal.pgen.0010033>
- 1540 Phelps, M. J., J. Liu, J. D. Benson, C. E. Willoughby, J. A. Gilmore
- 1541 *et al.*, 1999 Effects of Percoll separation, cryoprotective agents,
- 1542 and temperature on plasma membrane permeability character-
- 1543 istics of murine spermatozoa and their relevance to cryopreser-
- 1544 vation. *Biol. Reprod.* 61: 1031–1041. <https://doi.org/10.1095/biolreprod61.4.1031>
- 1545 Piálek, J., M. Vyskocilová, B. Bímová, D. Havelková, J. Piálková
- 1546 *et al.*, 2008 Development of unique house mouse resources
- 1547 suitable for evolutionary studies of speciation. *J. Hered.* 99:
- 1548 34–44. <https://doi.org/10.1093/jhered/esm083>
- 1549 Presgraves, D. C., 2010 The molecular evolutionary basis of spe-
- 1550 cies formation. *Nat. Rev. Genet.* 11: 175–180. <https://doi.org/10.1038/nrg2718>
- 1551 Reed, L. K., and T. A. Markow, 2004 Early events in speciation:
- 1552 polymorphism for hybrid male sterility in *Drosophila*. *Proc. Natl.*
- 1553 *Acad. Sci. USA* 101: 9009–9012. <https://doi.org/10.1073/pnas.0403106101>
- 1554 Rieseberg, L. H., and B. K. Blackman, 2010 Speciation genes in
- 1555 plants. *Ann. Bot. (Lond.)* 106: 439–455. <https://doi.org/10.1093/aob/mcq126>
- 1556 Sarver, B. A. J., S. Keeble, T. Cosart, P. K. Tucker, M. D. Dean *et al.*,
- 1557 2017 Phylogenomic insights into mouse evolution using a
- 1558 pseudoreference approach. *Genome Biol. Evol.* 9: 726–739.
- 1559 <https://doi.org/10.1093/gbe/evx034>
- 1560 Scopece, G., C. Lexer, A. Widmer, and S. Cozzolino,
- 1561 2010 Polymorphism of postmating reproductive isolation
- 1562 within plant species. *Taxon* 59: 1367–1374.
- 1563 Shorter, J. R., F. Odet, D. L. Aylor, W. Pan, C.-Y. Kao *et al.*,
- 1564 2017 Male infertility is responsible for nearly half of the ex-
- 1565 tinction observed in the mouse collaborative cross. *Genetics*
- 1566 206: 557–572. <https://doi.org/10.1534/genetics.116.199596>
- 1567 Shuker, D. M., K. Underwood, T. M. King, and R. K. Butlin,
- 1568 2005 Patterns of male sterility in a grasshopper hybrid zone
- 1569 imply accumulation of hybrid incompatibilities without selec-
- 1570 tion. *Proc. Biol. Sci.* 272: 2491–2497. <https://doi.org/10.1098/rspb.2005.3242>
- 1571 Snyder, R. L., 1967 Fertility and reproductive performance of
- grouped male mice, pp. 458–472 in *Comparative Aspects of Reproductive Failure*, edited by K. Benirschke. Springer-Verlag, New York https://doi.org/10.1007/978-3-642-48949-5_26
- Stamatakis, A., 2014 RAxML version 8: a tool for phylogenetic
- analysis and post-analysis of large phylogenies. *Bioinformatics*
- 30: 1312–1313. <https://doi.org/10.1093/bioinformatics/btu033>
- Streett, D. A., K. R. Petersen, A. T. Gerritsen, S. S. Hunter, and M. L.
- Settles, 2015 expHTS: analysis of high throughput sequence
- data in an experimental framework. *BCB* 15: 523–524. <https://doi.org/10.1145/2808719.2811442>
- Sweigart, A. L., and L. E. Fligel, 2015 Evidence of natural selec-
- tion acting on a polymorphic hybrid incompatibility locus in
- Mimulus*. *Genetics* 199: 543–554. <https://doi.org/10.1534/genetics.114.171819>
- Turner, L. M., and B. Harr, 2014 Genome-wide mapping in a
- house mouse hybrid zone reveals hybrid sterility loci and Dobz-
- hansky-Muller interactions. *eLife* 3: e02504.
- Turner, L. M., D. J. Schwahn, and B. Harr, 2012 Reduced male
- fertility is common but highly variable in form and severity in a
- natural house mouse hybrid zone. *Evolution* 66: 443–458.
- <https://doi.org/10.1111/j.1558-5646.2011.01445.x>
- Turner, L. M., M. A. White, D. Tautz, and B. A. Payseur,
- 2014 Genomic networks of hybrid sterility. *PLoS Genet.* 10:
- e1004162. <https://doi.org/10.1371/journal.pgen.1004162>
- Virdee, S. R., and G. M. Hewitt, 1994 Clines for hybrid dysfunction
- in a grasshopper hybrid zone. *Evolution* 48: 392–407.
- <https://doi.org/10.1111/j.1558-5646.1994.tb01319.x>
- Vyskočilová, M., Z. Trachtulec, J. Forejt, and J. Piálek, 2005 Does
- geography matter in hybrid sterility in house mice? *Biol. J. Linn.*
- Soc. Lond.* 84: 663–674. <https://doi.org/10.1111/j.1095-8312.2005.00463.x>
- Vyskocilová, M., G. Pražanová, and J. Piálek, 2009 Polymorphism
- in hybrid male sterility in wild-derived *Mus musculus musculus*
- strains on proximal chromosome 17. *Mamm. Genome* 20: 83–
91. <https://doi.org/10.1007/s00335-008-9164-3>
- Wang, R. J., A. Cécile, and B. A. Payseur, 2013 The evolution of
- hybrid incompatibilities along a phylogeny. *Evolution* 67: 2905–
- 2922.
- White, M. A., B. Steffy, T. Wiltshire, and B. A. Payseur,
- 2011 Genetic dissection of a key reproductive barrier between
- nascent species of house mice. *Genetics* 189: 289–304. <https://doi.org/10.1534/genetics.111.129171>
- Wright, K. M., D. Lloyd, D. B. Lowry, M. R. Macnair, and J. H. Willis,
- 2013 Indirect evolution of hybrid lethality due to linkage with
- selected locus in *Mimulus guttatus*. *PLoS Biol.* 11: e1001497.
- <https://doi.org/10.1371/journal.pbio.1001497>
- Yang, H., J. R. Wang, J. P. Didion, R. J. Buus, T. A. Bell *et al.*,
- 2011 Subspecific origin and haplotype diversity in the labora-
- tory mouse. *Nat. Genet.* 43: 648–655. <https://doi.org/10.1038/ng.847>
- Zheng, X., D. Levine, J. Shen, S. M. Gogarten, C. Laurie *et al.*,
- 2012 A high-performance computing toolset for relatedness
- and principal component analysis of SNP data. *Bioinformatics*
- 28: 3326–3328. <https://doi.org/10.1093/bioinformatics/bts606>

Communicating editor: D. Barbash

Genetics July (2018)
Author query sheet Larson (GEN_300840)

Do you want to participate in the Author's Choice Open Access option for your article?

- No
- Yes, Standard Open Access
- Yes, Creative Commons CC BY 4.0 License

Both Author Choice Open options make your article freely available to all readers (regardless of subscription) immediately after publication. With the Standard Author Choice Open Access, copyright remains with the Genetics Society of America as outlined in our copyright policy and future re-use of your content by others requires permission from GSA. With the CC BY 4.0 option, you hold copyright on the article, but anyone can share or adapt for any purpose, even commercially so long as they attribute the original source. Some authors have explained that they do not wish to grant others the right to modify and/or sell their content, so we offer both choices for the content to be made freely-available. Both Open Access options carry a surcharge of \$1500 for GSA members or \$2000 for non-members

More information: <http://www.genetics.org/content/after-acceptance#charges>

QA1 If you or your coauthors would like to include an ORCID ID in this article, please provide your respective ORCID IDs along with your corrections.

Note: If you do not yet have an ORCID ID and would like one, you may register for this unique digital identifier at <https://orcid.org/register>.

- 1** Please verify the affiliations are correct.
- 2** Please confirm the corresponding author's address.
- 3** Please check all figure legends carefully to confirm that any and all labels, designators, directionals, colors, etc. are represented accurately in comparison with the figure images.
- 4** Any alternations between capitalization and/or italics in genetic and taxonomic nomenclature have been retained per the original manuscript. Please confirm that all nomenclature has been formatted properly throughout. Per journal style, uppercase Greek letters should remain roman even when appearing in a term where the overall style is italic (e.g., a gene name such as *kap108Δ*). Note that headings are set all roman or all italics based on journal style and should not be changed.
- 5** Please verify all URLs in your article.
- 6** Please spell out HF in full as it only appears once in the text.
- 7** Please spell out QB3 in full at both instances in the text.
- 8** Please spell out minDP, maxDP, and minGQ at first use, followed by the abbreviations in parentheses.
- 9** Please spell out VCFs in the sentence beginning 'We generated a BED...'
- 10** Please spell out MPI in full as it is only used once in the text.
- 11** Please spell out GTR in full as it is only used once in the text.
- 12** Please spell out QD, FS, QUAL, ReadPosRankSum, and MQRankSum in full.
- 13** Please spell out MQ at first use, followed by the abbreviation in parentheses.
- 14** Please spell out QUAL in full in sentence beginning 'We parsed reads...'
- 15** Please provide URL for Li reference.
- 16** Please define AA and AB in the legend for Table 4.